THE REAL-TIME DIGITAL CONTROL OF A REGENERATIVE ABOVE-KNEE PROSTHESIS

By

KEITH AARON TABOR

B.S. Mech. Eng., Michigan Technological University
(1984)

SUBMITTED TO THE DEPARTMENTS OF
MECHANICAL ENGINEERING
and
ELECTRICAL ENGINEERING AND COMPUTER SCIENCE
IN PARTIAL FULFILLMENT OF THE REQUIREMENTS
FOR THE DUAL DEGREE OF

MASTER OF SCIENCE IN MECHANICAL AND ELECTRICAL ENGINEERING

at the

MASSACHUSETTS INSTITUTE OF TECHNOLOGY
May 1988

Signature of Author ..... Keith Aaron Tabor
Departments of Mechanical and Electrical Engineering
May 6, 1988

Certified by .....
Woodie Claude Flowers
Professor, Mechanical Engineering
Thesis Supervisor

Certified by .....
J. Kenneth Salisbury, Jr.
Research Scientist, A.I. Laboratory
Thesis Supervisor

Accepted by .....
Ain A. Sonin
Departmental Graduate Committee
Department of Mechanical Engineering

THE REAL-TIME DIGITAL CONTROL

OF A REGENERATIVE

ABOVE-KNEE PROSTHESIS

by

KEITH AARON TABOR

Submitted to the Departments of Mechanical Engineering
and of Electrical Engineering and Computer Science
on May 6, 1988 in partial fulfillment of the
requirements for the Degree of Dual Master of Science.

A B S T R A C T

Although much research has been directed toward knee prosthesis design, above-knee amputees still have much more difficulty walking than a normal. Active prostheses in the past have improved the walking ability of amputees but have not been designed to be self contained. A portable active prosthesis is desired.

Previous research resulted in the development of a self-contained, energy-regenerative, active prosthesis but a regenerative controller was needed. A controller for the regenerative knee was designed that simultaneously controlled the knee during the swing phase of level walking while also optimally recovering energy. The controller was called an impedance regulator because it controlled the effective linear viscous damping of the knee joint. Experimental trials without amputees were conducted that verified the operation of the controller. However, two major problems were discovered. The knee was both uncontrollable and inefficient during certain states of the system and the mechanical friction was too large. Suggestions for improving both of these areas were made.

Thesis Supervisor: Woodie C. Flowers
Title: Professor of
Mechanical Engineering

Thesis Supervisor: J. Kenneth Salisbury, Jr.
Title: Research Scientist,
A.I. Laboratory

ACKNOWLEDGEMENTS

Many people and several companies have played very important roles in this research. First of all, I would like to thank my friends in the biomechanics lab. Bart Seth and I became friends during long periods of time debugging electronic circuits and performing experiments. Dawei Qi, Peter Mansfield, Ralph Burgess, Bill Murray, Dov Adelstein, and my office mates Norman, Mike, Grace, Scott, Jeff, and Sue over the last four years have helped me immeasurably.

General Electric was kind enough to provide me with a fellowship for two full academic years that made this research possible. National Semiconductor, Motorola, and Analog Devices were very kind and donated many expensive integrated circuits for the research.

Woodie Flowers has been patient with me during the last four years--even when I changed my thesis topic. He has helped me many times without realizing it and has become a friend. Ken Salisbury has helped me attack some of the more obscure control problems related to this work and has always been eager to help as often as I needed it. He has also become my friend.

Last of all, I would like to thank the individual that has helped me most of all--my patient, lovely wife, Philecia. She put up with years of talking about my research that would usually put her to sleep. I love her.

D E D I C A T I O N

This work is dedicated to the memory of Mr. Joseph Blaske. I owe him much more than I can say. Although he greatly encouraged me to be a medical doctor, I think he would have been proud of this work...

TABLE OF CONTENTS

LIST OF FIGURES

Chapter One

INTRODUCTION AND BACKGROUND

The human locomotion system is truly remarkable. It has allowed man to walk, run, and climb mountains. However, when a leg was partially or completely destroyed, a large amount of mobility was lost. Crude artificial legs in the form of peg legs were used for centuries to partially replace normal leg operation.

In this century, leg prostheses have become much more advanced but still are not perfected. Modern research has shown that above-knee (A/K) amputees consume 20 to 100% more energy walking the same distance as a normal [1]. The effort required to walk is so extreme that some amputees do not even wear a prosthesis. Therefore, improved artificial legs should provide mobility without requiring large energy inputs.

The A/K amputee gait also tends to appear somewhat awkward and unnatural when compared with a normal. Figure 1-1 illustrates some of the differences. Three points are especially worth noting: the prosthetic knee remains locked in stance phase while the normal knee flexes and then extends, the prosthesis is not capable of power output, and the center of gravity of the body fluctuates vertically about twice as much when using the prosthesis. These aspects of A/K amputee locomotion result in increased energy consumption and/or unnatural gait. An engineering trade-off

Figure 1-1: NORMAL AND AMPUTEE GAIT

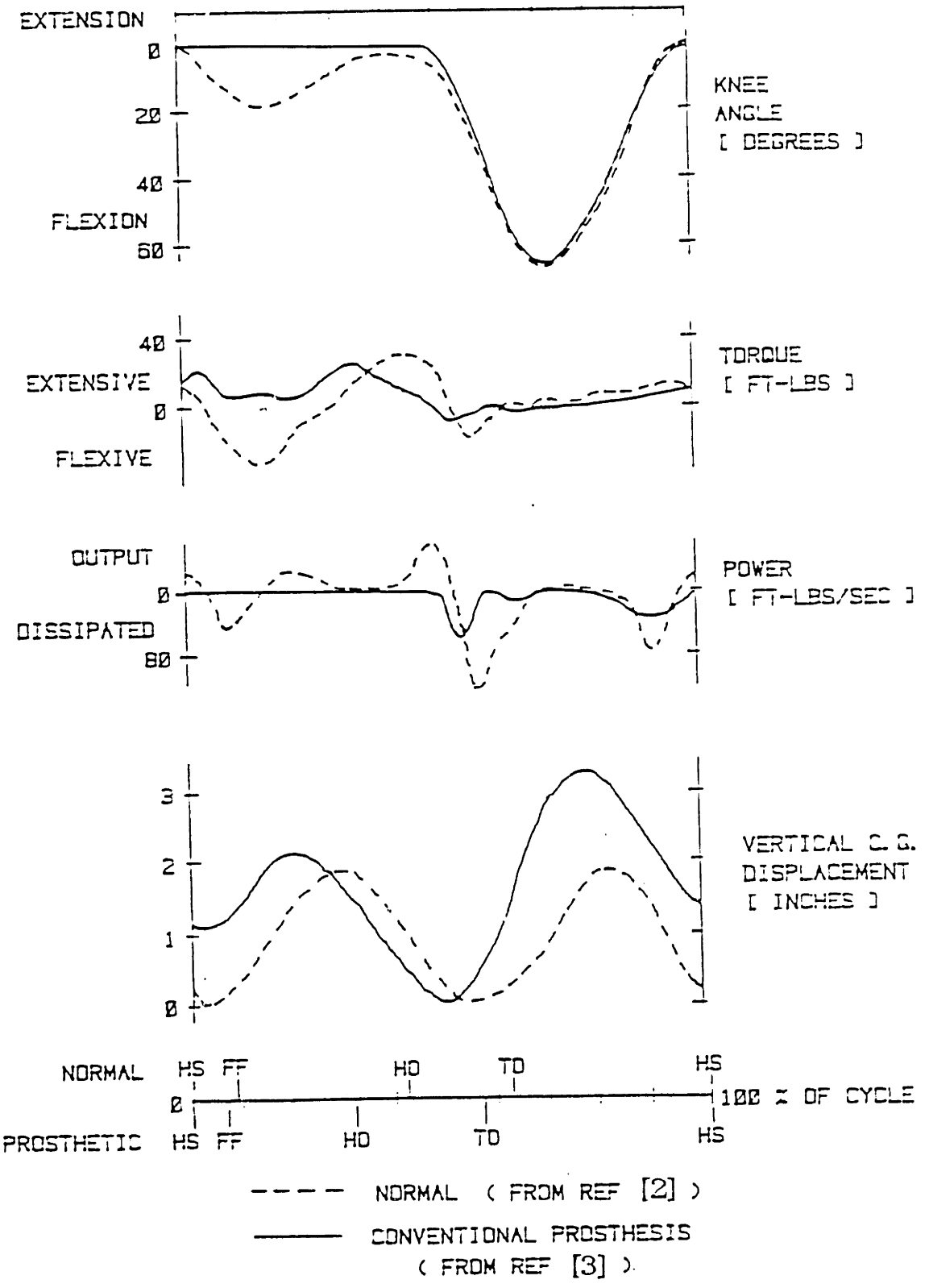

exists between the appearance of gait and energy consumption while walking. For instance, a skate-board-like prosthesis may radically reduce energy consumption while moving but it would hardly appear normal. In any case, a compromise must be obtained between desirable gait appearance and energy consumption.

Modern prosthetic legs generally contain the following parts: a knee mechanism, a "suction socket", a shank which connects the knee to the foot, and a solid-ankle cushioned-heel (SACH) foot. A "suction socket", which uses a vacuum to keep the socket and stump together, is usually used to hold the leg in position. The shank is simply a mechanical connection between the knee and foot. The SACH foot is the most commonly used ankle/foot combination. Much of the effort in prosthetic leg design is directed toward the knee.

All laboratory and commercially available leg prostheses fall into either the passive or active class. For our purposes, an active prosthesis will be defined as a prosthesis that can store energy and use it in an active or motor-like sense at a later time (the stored energy does not include, of course, the kinetic energy of the swinging prosthesis) while a passive device is the opposite--a device that cannot store energy.

Nearly all prostheses are passive. These prostheses, which are commonly used, can improve mobility but are somewhat limited. They range from crude mechanical devices to advanced electromechanical legs controlled by

microprocessors. Many offer no help in the stance phase of level walking, except for weight bearing, but make the swing phase better.

Active prostheses potentially have several advantages. They are required to implement the normal flex-extend motion of the knee during stance phase, which may lower energy consumption by reducing the vertical swing of the center of gravity if a new type of ankle/foot combination is used [4]. An active prosthesis is also more versatile since a passive knee can only use control schemes that dissipate energy. Finally, an active knee can also provide a more comfortable, natural, and controllable walk.

A universal active prosthesis, designed by Flowers [5], allowed many new control strategies to be tested. A new controller could be tried by simply writing a new computer program, without designing and building special mechanical and/or electrical hardware for a new knee. In this way, much time could be saved while designing future generations of knees. The hydraulic simulator allowed Grimes [6] and Stein [7] to experiment with active control schemes. The simulator could mirror the operation of any pinned-joint passive prosthesis. Since an external power source was required, the device was not intended to be portable.

Grimes and others noted that the knee, in a normal person during level walking, dissipated three to five times more energy than it required in an active or motor-like sense [8]. It was therefore possible to fully copy the

normal motion of the knee using energy regeneration. The normal leg motion could be mimicked using active control with no external power source, so the leg could be totally self-contained! It could recover the energy that would normally be dissipated in either a real or passive leg and use it later when needed.

Hunter designed and built the mechanical hardware of the first fully regenerative knee. The system consisted of a motor used both as a motor and a generator, a particle brake, a transmission, an amplifier, and the external enclosure. Hunter also concluded that a particle brake was needed to achieve maximum energy regeneration during level walking. A standard shank and SACH foot were used. Further detail can also be found in Hunter's thesis [9].

Hunter's work was the first in a series of projects done on the regenerative leg. Three visiting students from France; Sedbon, Cavril, and Marchand, assisted in software development (see the reference below). Seth studied energy regeneration and adapted the leg to do related experiments [10]. He was concerned with how energy could be optimally extracted from a generalized actuator. He was the first to control the regenerative knee by using a computer program.

The goal of this thesis is to explain how to control the regenerative, active knee prosthesis such that the swing phase of gait is acceptable while simultaneously recovering the largest amount of energy possible. Generally, maximum energy regeneration and desirable gait are conflicting

goals, since improving one usually reduces the performance of the other. A controller was developed that will mimic a linear viscous damper while recovering energy, since linear viscous damping control of knees has already been used to obtain acceptable gait.

This thesis is divided into six chapters. The second chapter is dedicated to an overview of the regenerative knee and explains its operation in detail. In chapter three, a model and control scheme are developed that implement the "impedance" control. Chapter four explains how optimal energy regeneration is included in the model and controller of chapter three. The fifth chapter presents experimental results from the nonoptimized control method. The conclusions and suggestions for future work are included in the final chapter.

Chapter Two

An Overview of the Regenerative Knee

In this chapter, the major components of the regenerative knee will be reviewed first, then detailed information on each component will follow.

The knee prosthesis can be divided into four major functional groups: the motor/generator system, the magnetic-particle brake system, the control system, and the energy storage system. A conceptual diagram is shown in Figure 2-1. Thick lines between blocks represent power flow while thin lines represent information exchange. The motor/generator system transforms mechanical energy into electrical energy, which is transferred to the energy storage element, or vise-versa. The magnetic-particle brake consumes a small amount of electrical energy while dissipating mechanical energy at a rate determined by its amplifier. The amplifiers, which control the motor and particle brake, are directly controlled by the microcomputer controller when running the desired control program. Each of these systems, which encompass the complete knee, will be described in detail below.

The motor system is comprised of the following parts: the motor itself, the mechanical transmission, and amplifier.

A DC permanent magnet motor rated at 1.18A and 145 oz-in. is used. It is connected to the knee axis through an

FIGURE 2-1: BLOCK DIAGRAM OF REGENERATIVE KNEE

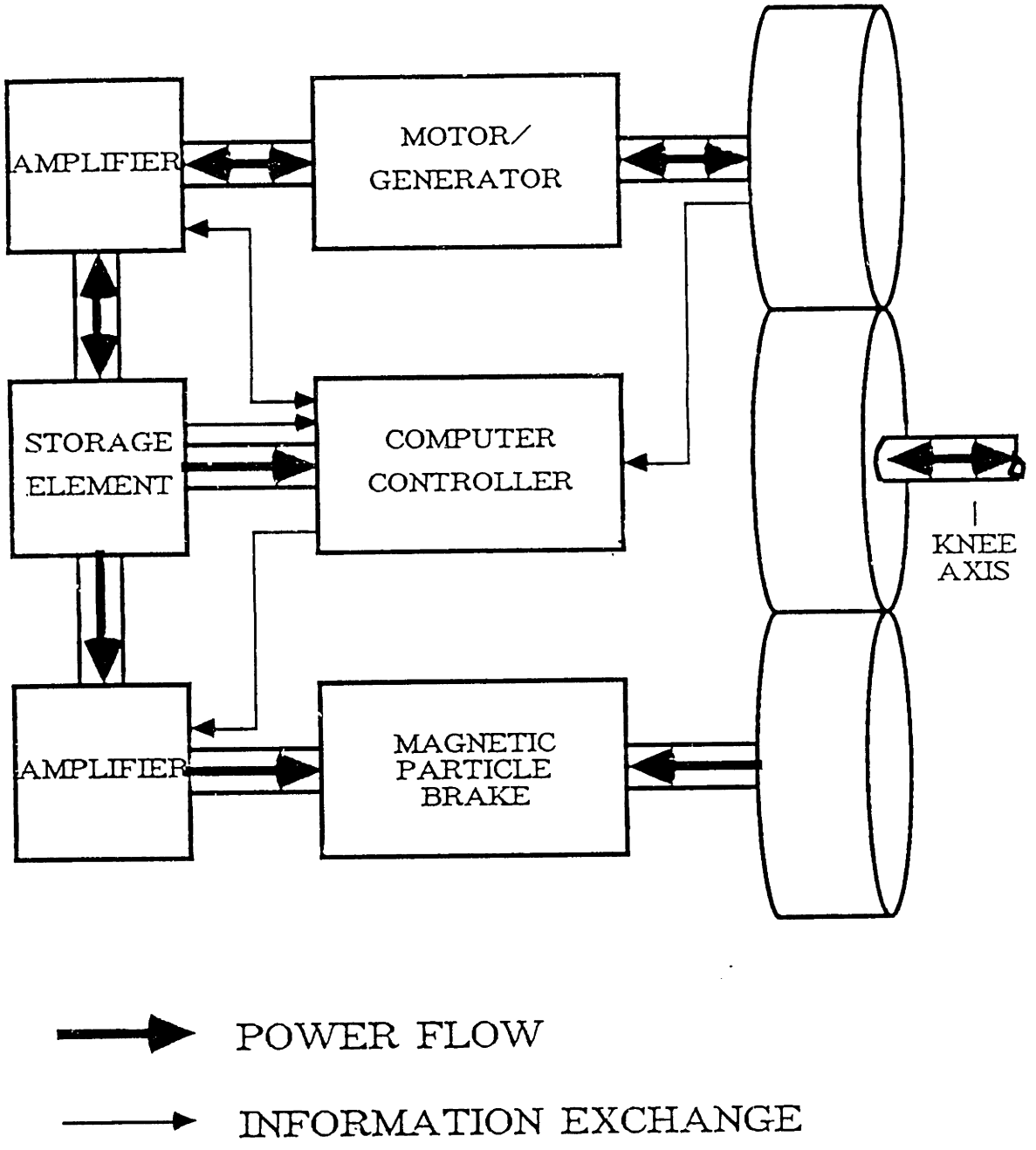

18:1 transmission composed of a belt and gears. The motor operates as either a motor or a generator depending on the amplifier quadrant. Further detail is provided by Hunter [9].

The motor is controlled by a bipolar, H-bridge, pulse-width-modulated (PWM) amplifier with a switching frequency of 20KHz. The PWM amplifier quadrant controls the direction, and the duty cycle the rate, of energy transfer between the motor/generator and storage element. The voltage supply used in most PWM motor circuits is replaced by a capacitor, which is the energy storage element (see Figure 2-2). The top FETs (A and C) are MOSFETs while the lower FETs (B and D) are SENSEFETs (a type a MOSFET with nearly lossless current sensing capability). The operation of the MOSFETs and SENSEFETs, used in these circuits, can be thought of as simple switches that are either on, with some small resistance, or off, with nearly infinite resistance. The PWM amplifier allows four distinct quadrants of motor/generator operation: motor +, motor -, generator +, and generator -. The plus and minus signs indicate the direction of motor rotation. In each quadrant, three things occur: one SENSEFET is on (conducting) continuously, another SENSEFET or MOSFET is intermittently switched on and off with a given duty cycle, and one diode is conducting part of the time (the table accompanying Figure 2-2 explains which diode, SENSEFET(s), and MOSFET, if any, are used in each quadrant). The switching of one SENSEFET or MOSFET results

FIGURE 2-2: MOTOR/GENERATOR CIRCUIT AND OPERATION

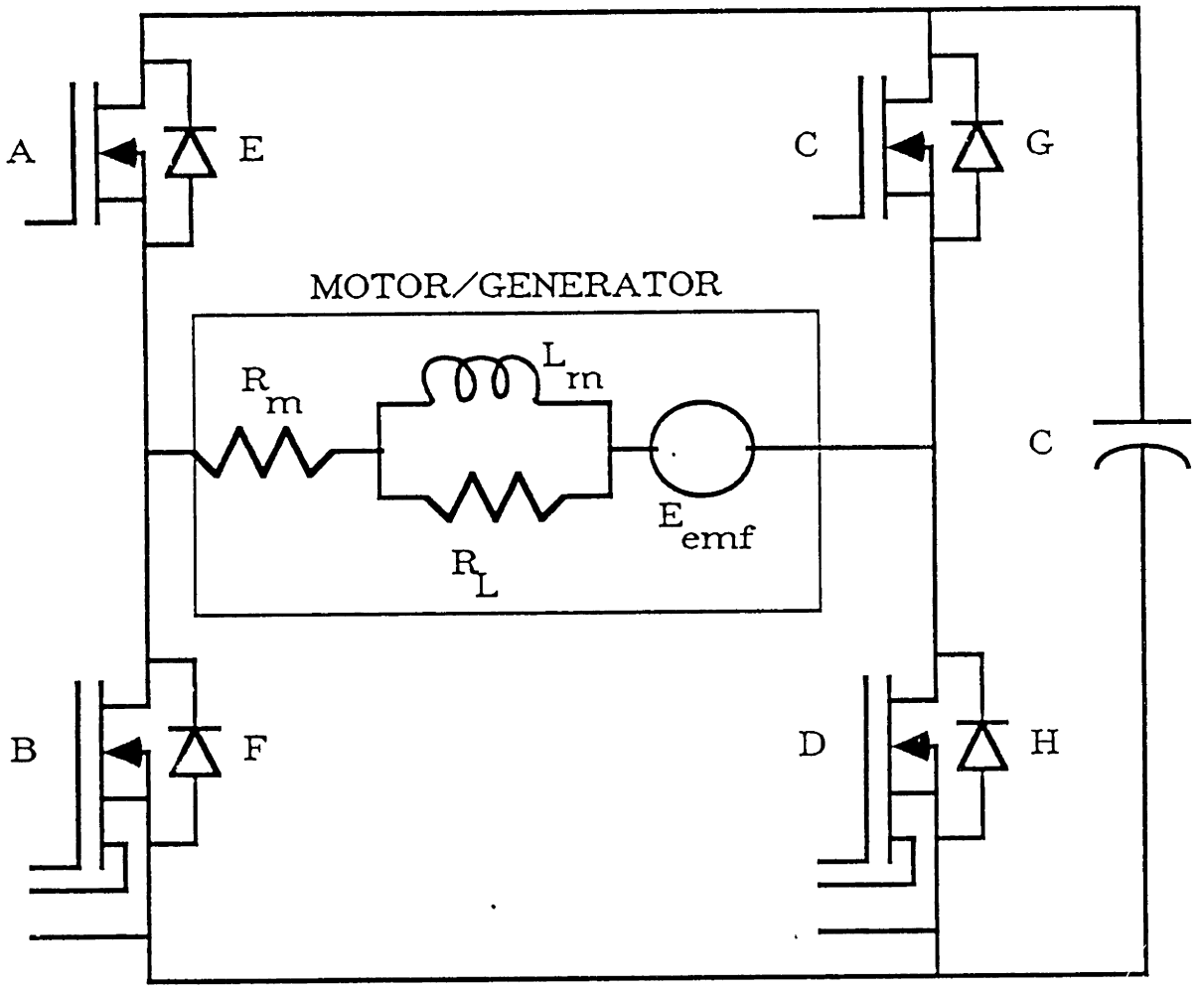

	MOS/SENSEFET		
Quadrant	Switching	On	Conducting Diode
Motor +	A	D	F
Generator +	B	D	E
Motor -	C	B	H
Generator -	D	B	G

Note: A, C are MOSFETs; B, D are SENSEFETs.

in two distinct circuits for each quadrant, one when the FET is conducting and one when it is not.

In the motor quadrants, an average voltage adjustable between zero and the full capacitor voltage is applied across the motor by varying the duty cycle. Therefore, the motor is periodically switched from being connected to the capacitor to being shorted by the small on resistance of the SENSEFET and a diode (see Figure 2-3 where the motor + circuits are shown). The relative amount of time each of the circuits is operational depends on the duty cycle.

The generator quadrants are similar to the motor quadrants with the exception that energy is flowing into the capacitor instead of out of it. The generator current is forced to flow either through the low resistance path of the SENSEFETs or into the capacitor (see Figure 2-4 where the generator + circuits are shown). The generator can charge the capacitor even when the capacitor voltage is larger than the motor back emf (E_{emf}) because of the large voltages created by the switched motor inductance!

Therefore, the motor is controlled by the PWM amplifier allowing energy to flow into the knee system or out of it at variable rates.

The magnetic-particle brake system includes the particle brake itself, an amplifier, and a belt that connects the brake to the motor transmission (providing a 36:1 reduction from the brake to the knee axis). The particle brake produces a resistive torque proportional to

FIGURE 2-3: MOTOR QUADRANT EQUIVALENT CIRCUIT MODELS

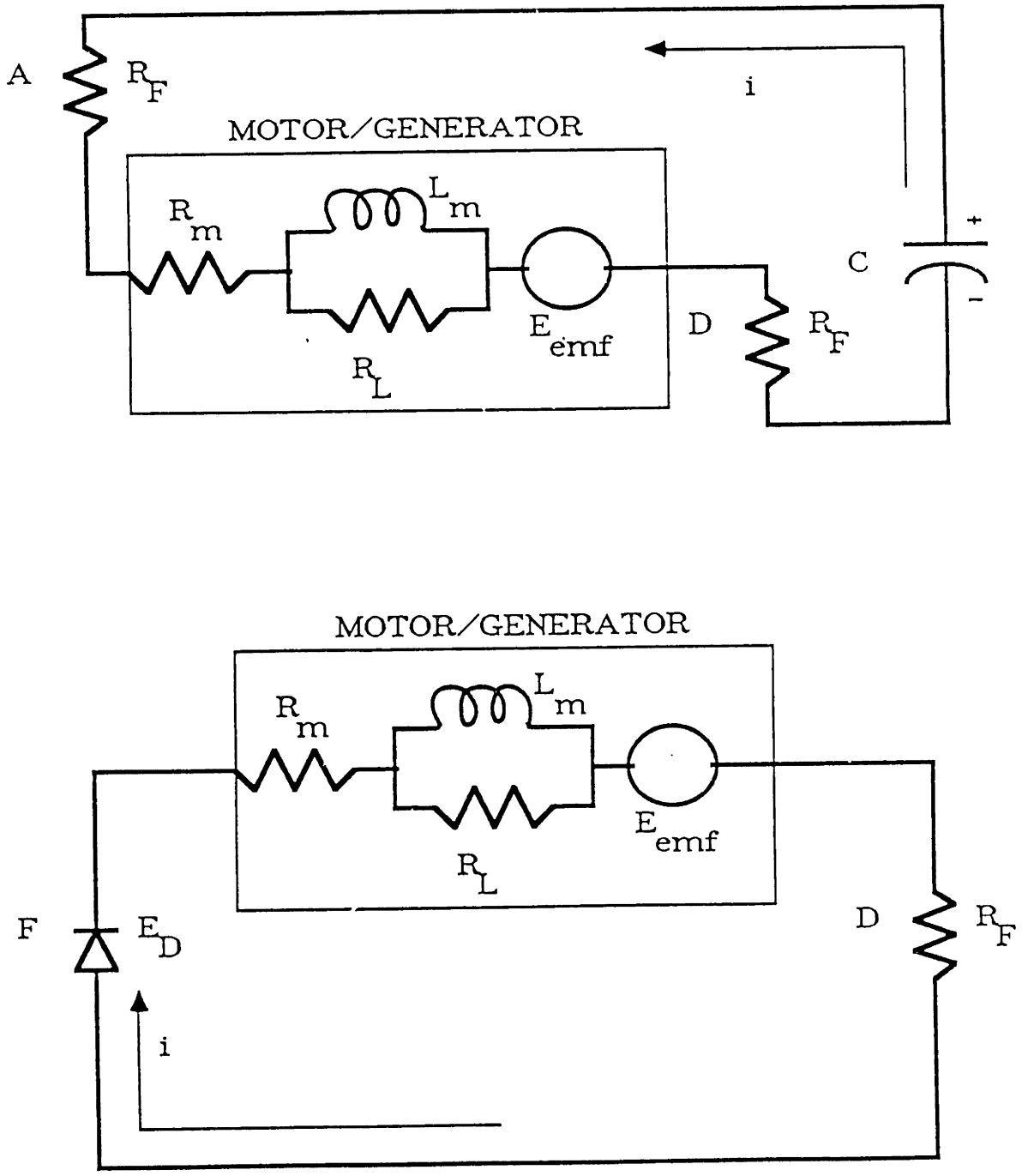

FIGURE 2-4: GENERATOR QUADRANT EQUIVALENT CIRCUIT MODELS

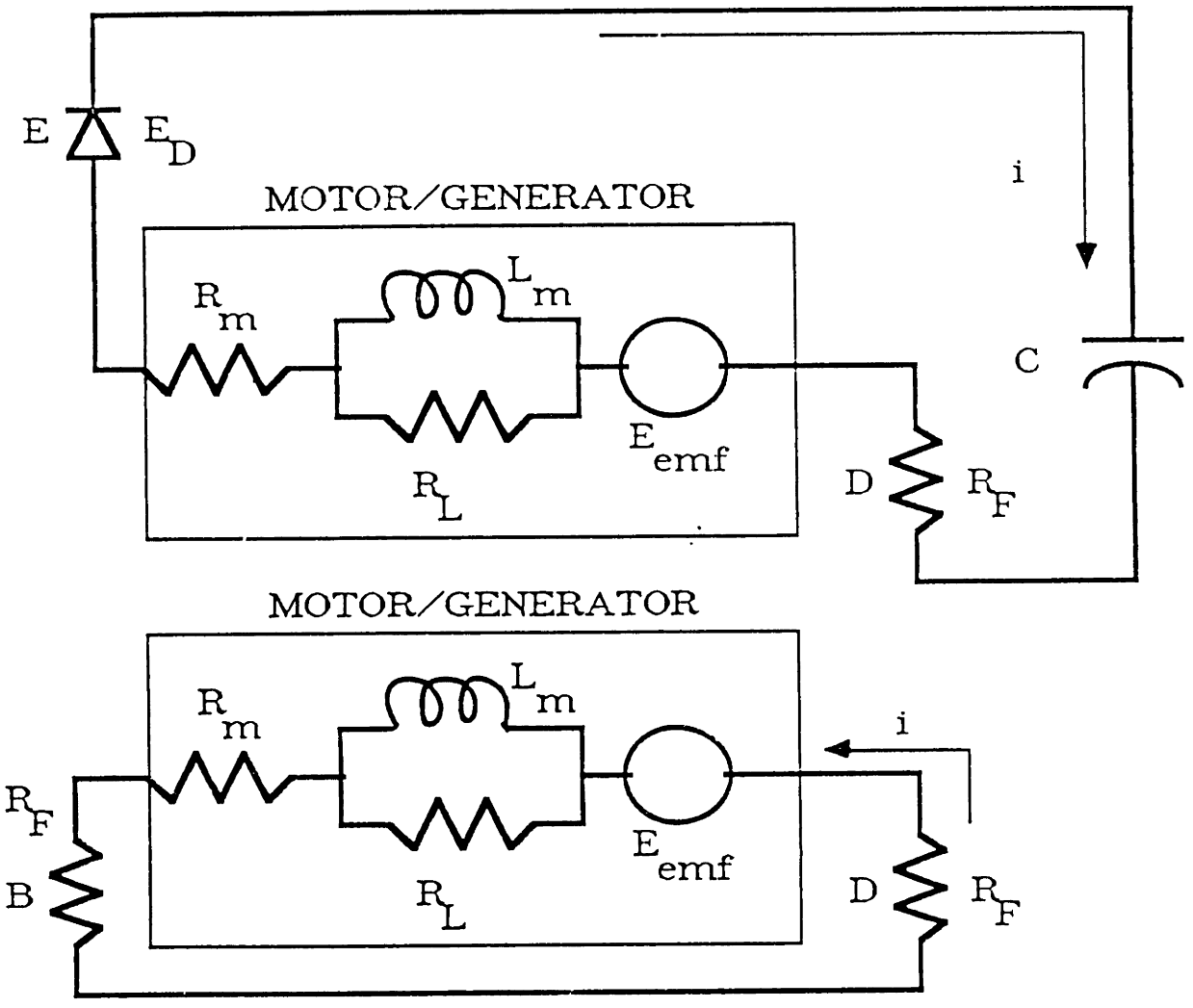

FIGURE 2-5: MAGNETIC PARTICLE BRAKE CIRCUIT

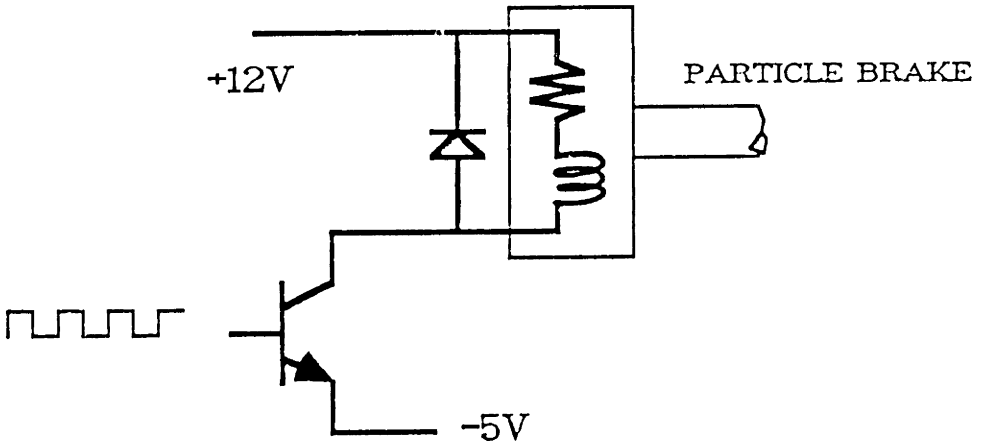

the current flowing through it. It also allows the knee to be locked securely. A simplified particle-brake amplifier circuit, which uses a pulse-width-modulated NPN transistor, is shown in Figure 2-5.

The controller group, which includes the microcomputer and transducers, comprises the third major functional block of the knee. A NSC800 microprocessor running at 4 MHz is the brain of the controller. The computer reads the various transducers, executes the control algorithm in real time, and then selects the proper duty cycle for the brake, and the proper duty cycle and quadrant for the motor/generator. The control program is written in machine language, so a new control method can be created by simply changing the software. The microprocessor is also used to record experimental data. The following four sensors are used in the knee: a optical encoder (mounted on the motor) for angular position measurement, from which angular velocity information is derived, SENSEFETs for motor current measurement, a capacitor voltage sensor, and a torque transducer at the knee axis.

An electrolytic capacitor rated at 2200MF and 75 volts is used to store the recovered electrical energy. It supplies the energy to motor the leg when needed. The capacitor will also supply the energy needed for the computer and particle brake in the future, but at this time both are powered by an external power supply.

Each of the four functional groups described above must interact effectively with each other in order to create an efficient, working regenerative knee. A mathematical model and a effective controller will be the subject of the next chapter.

Chapter Three

System Modeling and Control

The objective of this chapter is to explain how an effective controller for the regenerative knee was developed. First of all, the term, impedance regulator, will be defined. Next, the choice of an impedance regulator will be explained and its operation described. It will be shown that the creation of a current servo is a critical part of the development of an impedance regulator. Circuit models will be used to develop a mathematical model that predicts motor current. Then, the current servo control program will be defined using this mathematical model. Finally, the limitations of the regulator will be explained.

In this thesis, a controlled device which develops a resistive torque (opposing the direction of motion) linearly with velocity will be called an "impedance" regulator or a linear viscous damper. This type of controller, when capable of regenerating energy, will be called a regenerative, impedance regulator.

An impedance regulator was chosen for the following three reasons: a previous prosthesis which used this type of control (linear viscous damping) has improved the swing phase of level walking [11], this type of control is easily adapted to energy regeneration, and it is simple. Knees that use viscous damping "control" range from relatively simple mechanical devices to complex apparatuses that use

computer-controlled, magnetic-particle brakes similar to the one used in the regenerative knee [12]. Nonetheless, it should be noted that several types of nonlinear damping schemes have been used and could be easily adapted to the regenerative knee. At any rate, all previous devices, while acting as rotational viscous dampers, have not regenerated energy during swing phase.

The impedance regulator algorithm is composed of the following general steps: the knee velocity is measured, the resistive torque is computed that achieves the desired viscous damping or impedance coefficient, the generator current (and possibly also the particle brake current) necessary to produce this resistive torque is determined, the motor quadrant and duty cycle(s) are determined which will result in this current (or currents), and the resulting command signals are sent.

The regenerative knee can generate a resistive torque in five different ways: by the generator alone ("motor" and "generator" refer to a singe device operating as a motor or as a generator, respectively), by the particle brake alone, by the generator and particle brake, by the motor alone, or by the motor and particle brake. Obviously, to recover energy, the generator must be used at least some of the time. It is always more efficient to use the particle brake to develop opposing torque than to use the motor, so the motor will never be used in the impedance regulator because it reduces stored energy faster. Since regeneration is

desired, only the modes of operation that include the generator will be considered.

In this chapter, an impedance regulator, which does not use the particle brake, will be defined. A block diagram of the controller, without particle brake, is shown in Figure 3-1. The resistive torque generated by the DC permanent magnet motor electronics is called the electrical resistive torque (T_e). This torque is linearly related to the motor/generator current ($T_e=K_T i$). The real mechanical, viscous frictional or impedance coefficient (b_m, where $T_m=b_m w$) can always be added to the electrical viscous coefficient (b_e) to obtain an overall system impedance coefficient (b_n, ie. $b_n=b_m+b_e$). Nonetheless, designing the current servo control program is the most difficult task in realizing the impedance regulator.

A model of the generator quadrants is required before a current servo control program can be designed. The model must relate the inputs of the current servo control program; knee angular velocity, capacitor voltage, and motor current to their outputs; duty cycle and quadrant. Due to the symmetry of the power electronics, one model will suffice for both generator directions. The specific generator quadrant in use is determined simply by the direction of rotation of the knee. A circuit model, valid for both the generator + and generator - quadrants, is shown in Figure 3-2. (The motor magnetic losses, shown schematically in Figures 2-3 and 2-4 as a resistance, R_L, in parallel with

FIGURE 3-1: IMPEDANCE REGULATOR BLOCK DIAGRAM

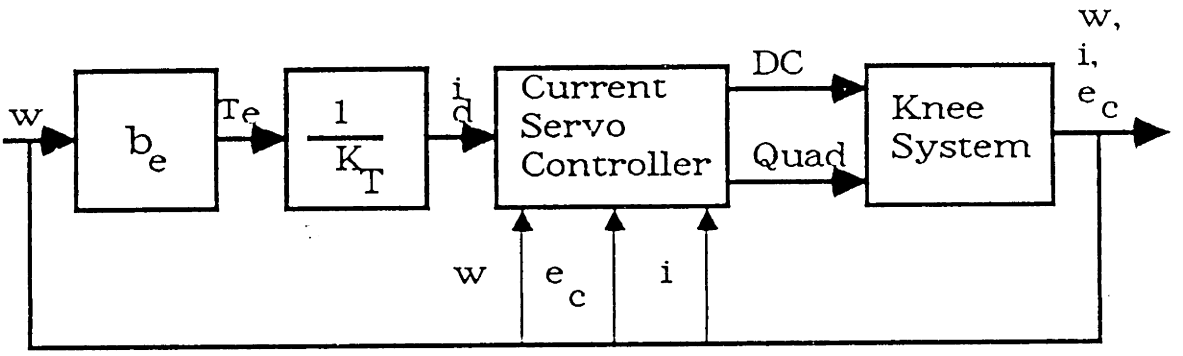

FIGURE 3-2: CIRCUIT MODEL FOR GENERATOR QUADRANTS

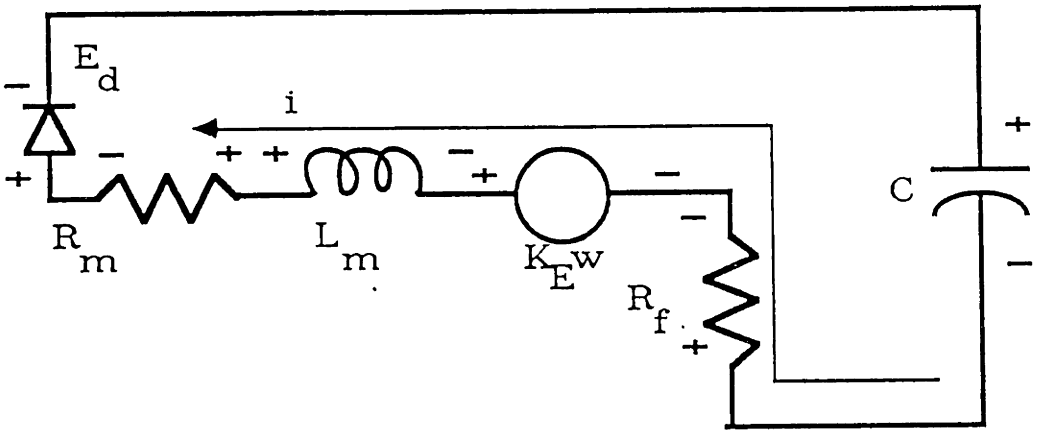

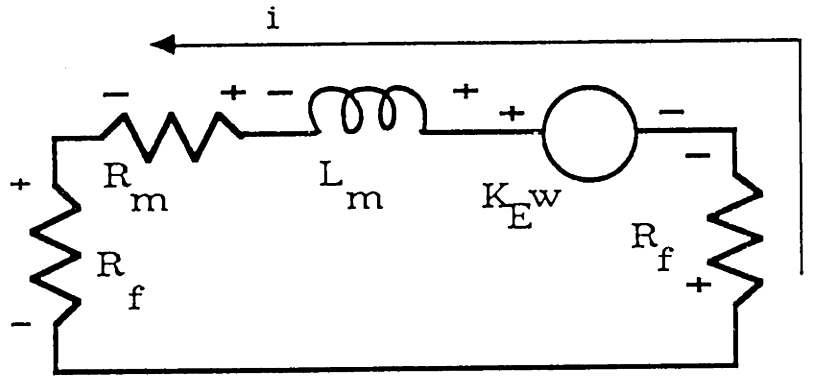

the motor inductance, is ignored in the following steady-state derivation because it is usually five to ten times larger than R_M.) The current flows through the top circuit when the switched SENSEFET (B or D) is open and current flows through the bottom circuit when the switched SENSEFET is closed (or conducting). Therefore, a duty cycle (DC) of unity means that the bottom circuit is always in operation while a duty cycle of zero means that the top circuit is always in operation. When the duty cycle is not zero or one, each circuit is in operation part of the time. This results is a time weighted averaging of the circuits.

The equations describing the top and bottom circuits, respectively, follow:

$$-E_C - (R_F + R_M + L_M s)i + wK_E - E_D = 0. \quad (3\text{-}1)$$

$$-(2R_F + R_M + L_M s)i + wK_E = 0. \quad (3\text{-}2)$$

where,

E_C = capacitor voltage,
R_F = SENSEFET on resistance,
R_M = motor resistance,
L_M = motor inductance,
i = motor current,
w = knee angular velocity,
K_E = motor voltage constant,
E_D = diode voltage drop, and
s = derivative operator.

The term wK_E is equivalent to E_{emf}, the motor back emf. A quasistatic assumption is now made--it is assumed that at any given instant of time, the capacitor voltage and knee angular velocity are changing at a negligible rate with respect to the control frequency. Also, it is assumed that the system is linear and time invariant (LTI).

Equations (3-1) and (3-2) are first solved for the motor current.

$$i = \frac{wK_E - (E_C + E_D)}{(R_F + R_M + L_M s)}. \tag{3-3}$$

$$i = \frac{wK_E}{(2R_F + R_M + L_M s)}. \tag{3-4}$$

Since a steady-state equation is desired, the derivative operator, s, is set to zero. Equation (3-3) is multiplied by (1-DC) and equation (3-4) is multiplied by DC and then combined using the assumption that R_F is small compared to R_M. Implicit in the combination of these equations, is the assumption that the switching time between circuits is negligible and that their time constants are almost identical.

$$i = \frac{wK_E - (E_C + E_D)(1 - DC)}{(R_F + R_M)}. \tag{3-5}$$

For reference, it is also desirable to have an equation for the electrical impedance coefficient (b_e). It is shown below:

$$b_e = \frac{K_T K_E}{(R_F + R_M)} - \frac{K_T(E_C + E_D)(1 - DC)}{w(R_F + R_M)}. \tag{3-6}$$

The final step in the derivation consists of solving equation (3-5) for the DC.

$$DC = \frac{(R_F + R_M)i - wK_E}{(E_C + E_D)} + 1. \tag{3-7}$$

Equation (3-7) is the desired relation between the duty cycle and the motor current.

The impedance regulator shown in Figure 3-1, with the current servo controller box filled with equation (3-7), should yield very good performance with only two exceptions. First, a nonlinear clipping is sometimes present that results in a different current than predicted by the model. In the knee prosthesis, this effect is observable but not too severe. Second, the knee is sometimes uncontrollable due to insufficient capacitor voltage. This sometimes creates a serious problem. Fortunately, both of these problems can be greatly reduced or even eliminated.

A nonlinear clipping occurs due to the diode. See Figure 3-2. The diode only allows current to charge the capacitor, as desired for regeneration. However, it also causes nonlinearities that are not modeled--resulting in a deviation between the actual and predicted current. Consequently, the current servo becomes less accurate.

The clipping effect can be better understood by closely examining each generator circuit.

When the top circuit is in operation (Figure 3-2), the motor back emf ($K_E w$) is opposed by the capacitor voltage, causing the motor current to decrease with time. If the capacitor voltage is larger than the motor back emf, the diode may become intermittently reverse biased or turned off, causing the motor current to stop. However, the model does not exclude negative current flow through the diode, so it predicts an incorrect motor current, always smaller than the actual current.

When the bottom circuit is operative, the motor is effectively shorted by the small on resistances of the SENSEFETs (R_F), causing the motor current to increase. The capacitor voltage is not opposing the back emf of the motor is this case. To prevent clipping, it must increase the motor current to a sufficient level so that it does not go to zero in the other circuit.

The switching between the two circuits results in current ripple at the switching frequency of 20KHz. The larger the current ripple, the larger the chance that nonlinear clipping will occur.

The electrical time constant of the motor is related to the amount of current ripple present. Figure 3-3 shows how the motor current varies at the PWM amplifier switching frequency of 20KHz without clipping. Figure 3-4 shows the "actual" dynamic motor current and the "actual" average motor current during clipping. The predicted average motor current (from equation (3-5)) would be zero or even less than zero in this case. Therefore, the "actual" average motor current is always larger than predicted when clipping is occurring.

Increasing the electrical time constant (T_E) will reduce the current fluctuation--reducing the possibility of clipping and the amount of it when present. The electrical

Figure 3-3
DYNAMIC VARIATION OF MOTOR CURRENT
WITHOUT CLIPPING

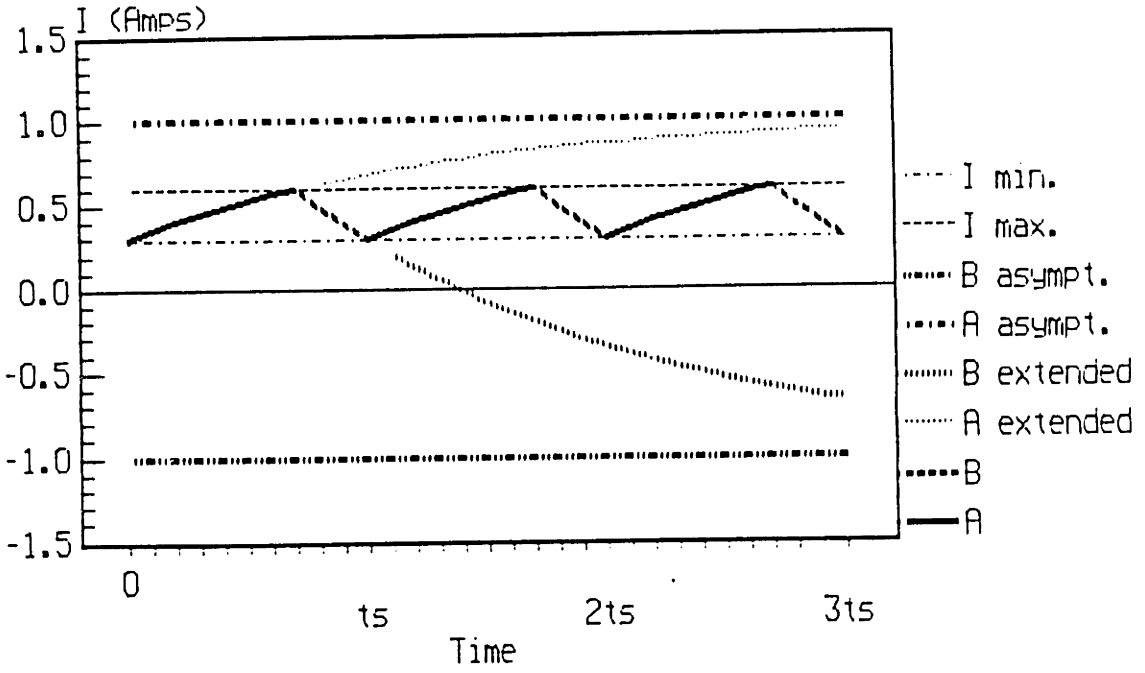

Notes: 1) "A" represents the motor current, when the circuit shown in the bottom of figure 3-2 is operational, for a period of time (DC)ts.

2) "B" represents the motor current, when the circuit shown in the top of figure 3-2 is operational, for a period of time (1-DC)ts.

3) "A asympt." represents the steady-state motor current, when DC=1.0, which can be actually realized.

4) "B asympt." represents the steady-state motor current, when DC=0.0, which can not be actually realized. (One FET acts like a diode preventing negative current flow in this case.)

5) A duty cycle of about 0.7 is shown.

6) "ts" is the switching period of the PWM amplifier.

7) The motor current variation and time constants were chosen for the purposes of illustration only and do not represent typical values!

Figure 3-4
DYNAMIC VARIATION OF MOTOR CURRENT
WITH CLIPPING

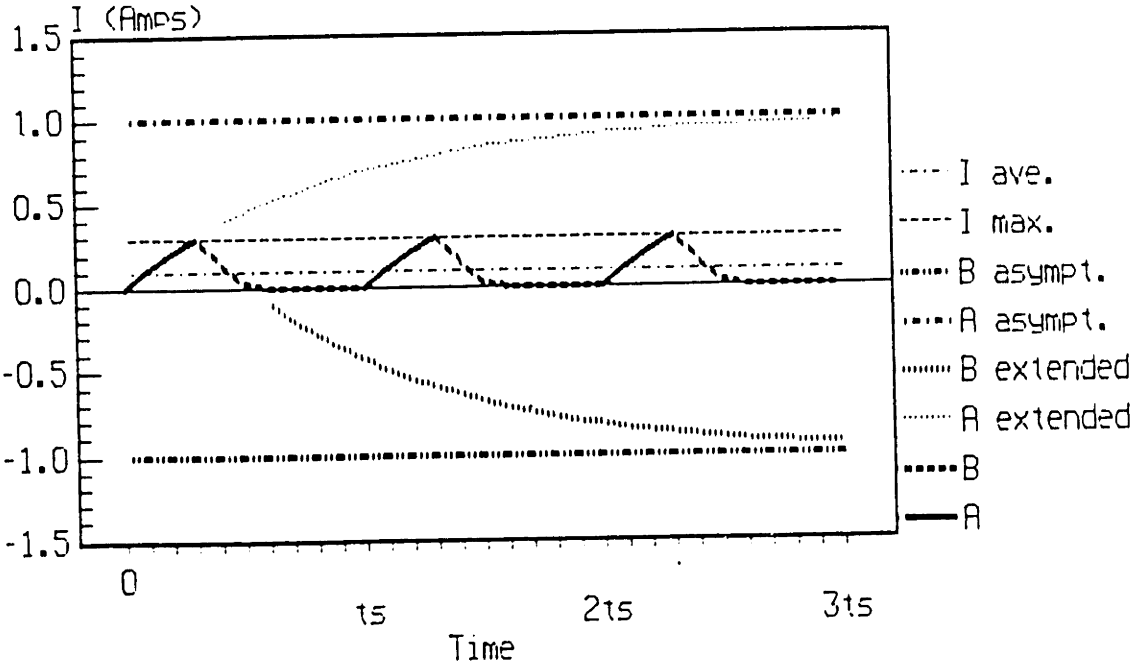

Notes: 1) "A" represents the motor current, when the circuit shown in the bottom of figure 3-2 is operational, for a period of time (DC)ts.

2) "B" represents the motor current, when the circuit shown in the top of figure 3-2 is operational, for a period of time (1-DC)ts.

3) "A asympt." represents the steady-state motor current, when DC=1.0, which can be actually realized.

4) "B asympt." represents the steady-state motor current, when DC=0.0, which can not be actually realized. (One FET acts like a diode preventing negative current flow in this case.)

5) A duty cycle of about 0.3 is shown.

6) "ts" is the switching period of the PWM amplifier.

7) The motor current variation and time constants were chosen for the purposes of illustration only and do not represent typical values!

8) In this case, the model predicts zero motor current when in fact there is a nonzero motor current, as shown above (I ave. > 0).

time constant is approximately related to the motor inductance and resistance as follows:

$$T_E = \frac{L_M}{R_M}. \qquad (3\text{-}8)$$

Therefore, increasing the motor inductance and/or decreasing the motor resistance will result in a longer electrical time constant and reduced clipping--reducing the nonlinear deviations from equation (3-5). An external inductor could be added in series with the motor to increase the electrical time constant.

Two other possible solutions to this problem exist. The PWM amplifier could be switched at a higher frequency with an associated loss in efficiency and/or current feedback could be used.

Clipping has a tendency to occur when the capacitor voltage is large, the knee angular velocity is small, and the duty cycle is small but not zero.

The knee system is also uncontrollable during a certain state of the system. When the capacitor voltage is near zero, the top and bottom circuits shown in Figure 3-2 are identical, with the exception that a diode is replaced by the SENSEFET on resistance (R_F). Under this condition, the current is nearly independent of the duty cycle. A small motor current is not possible, so a larger current, and hence, electrical impedance (since $b_e=K_T i/w$) than desired results. However, as the capacitor charges, this uncontrollability problem disappears. Figures 3-5 and 3-6

Figure 3-5
MINIMUM MOTOR CURRENT AS A FUNCTION OF
ANGULAR VELOCITY AND CAPACITOR VOLTAGE
(DC=0.0)

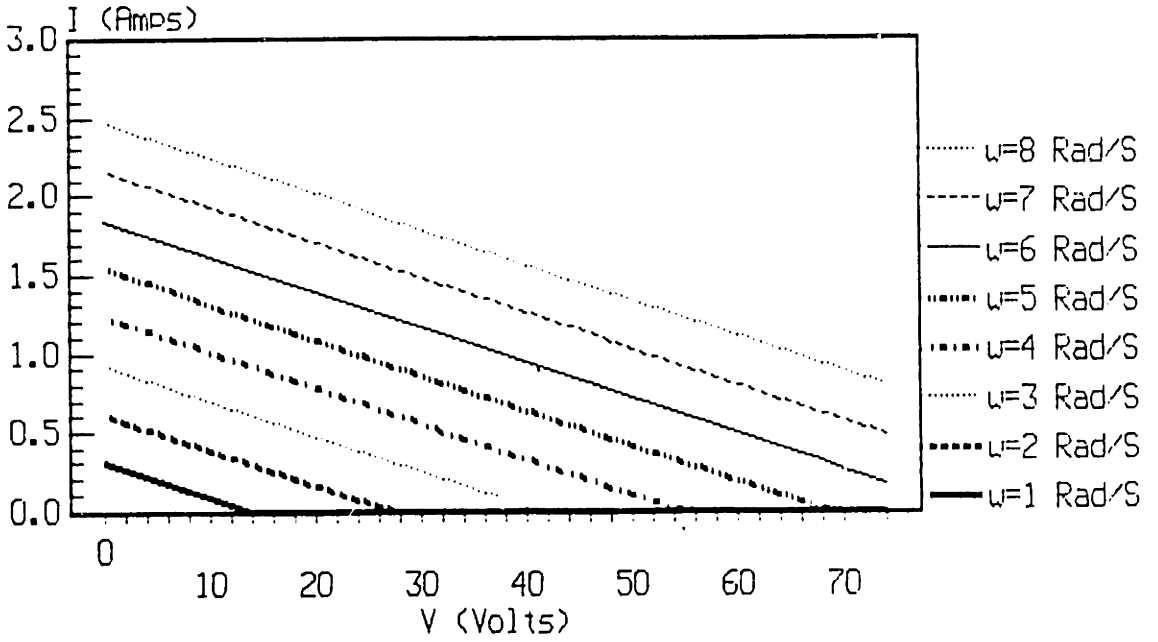

Figure 3-6
MINIMUM MOTOR CURRENT AS A FUNCTION OF
CAPACITOR VOLTAGE AND ANGULAR VELOCITY
(DC=0.0)

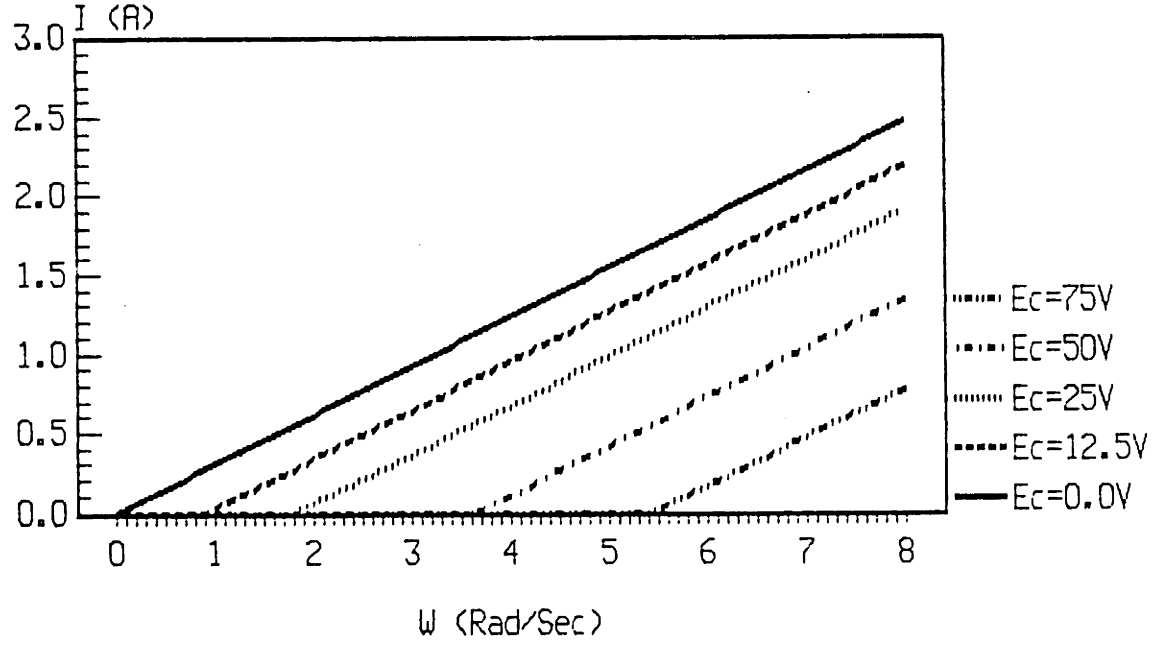

Figure 3-7
AVAILABLE VISCOUS DAMPING AS A FUNCTION
OF ANGULAR VELOCITY AND CAPACITOR VOLT.
(DC=0.0)

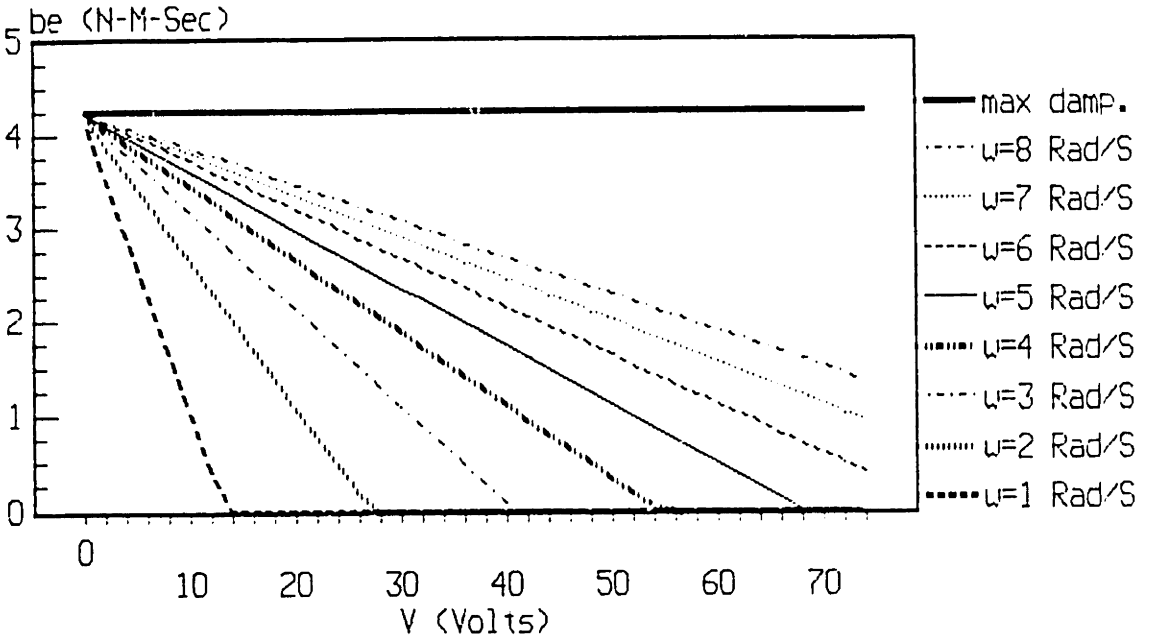

Figure 3-8
AVAILABLE VISCOUS DAMPING AS A FUNCTION
OF CAPACITOR VOLT. AND ANGULAR VELOCITY
(DC=0.0)

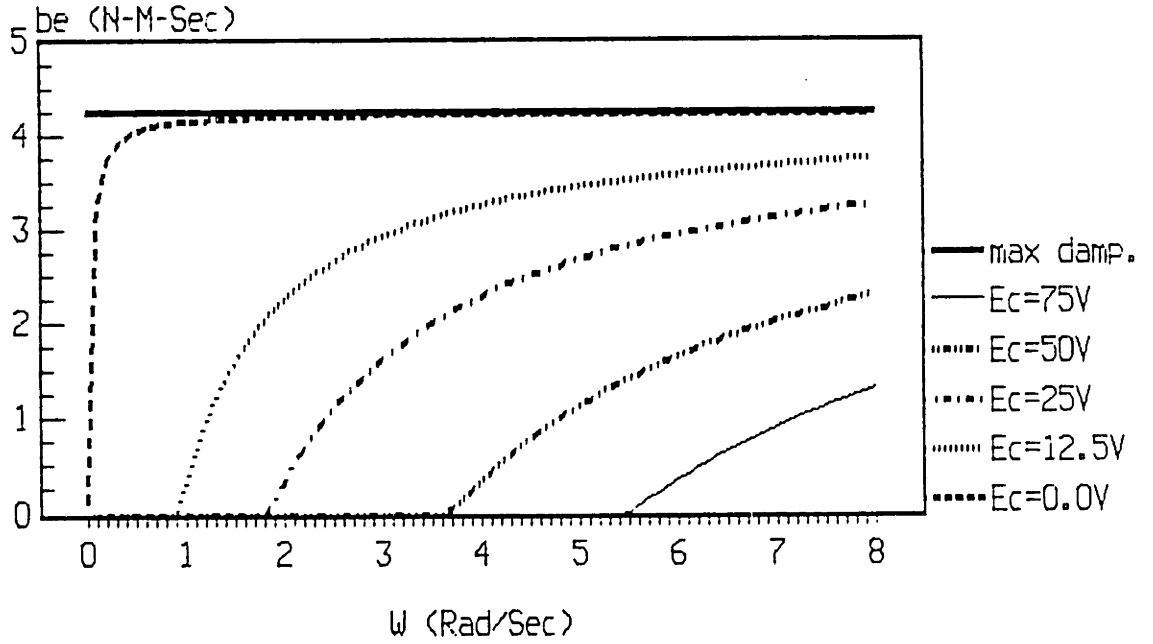

show that a small current cannot be obtained when the capacitor is nearly discharged, especially when the angular velocity of the knee (w) is large. Figures 3-7 and 3-8 show a related fact, that a small impedance cannot be obtained under the same conditions. These figures are plots of the same information displayed in different ways. The data were computed from equations (3-5) and (3-6). In Figures 3-7 and 3-8, the achievable range of impedances lie between the top horizontal line and the given lower curve.

The uncontrollability problem can be completely avoided, except at start-up, by never letting the capacitor voltage become discharged below about 60 volts. Thus, the faster the leg moves and the lower the desired impedance level is, the larger the capacitor voltage must be to achieve complete controllability.

The regenerative impedance regulator shown in Figure 3-1 was the complete regulator desired. Equation (3-7) mathematically defined the current servo. The regulator algorithm was written in machine language to allow the regenerative knee to function like a linear viscous damper.

In summary, the choice of an impedance regulator has been explained, impedance regulation has been defined and its operation described. The development of a current servo was found to be an essential step towards the development of the entire controller. A circuit model and its mathematical

description were obtained to predict motor current. The model limitations and methods mitigating these limitations were discussed. In the following chapter, optimal energy regeneration issues will be investigated.

Chapter Four

Optimal Energy Regeneration

In this chapter, an optimal energy regeneration scheme will be developed that can function with the nonoptimal impedance regulator described in the previous chapter. First, several definitions will be presented to aid in understanding the derivations in this chapter. Next, it will be shown that if a net impedance coefficient is chosen for best swing phase control then maximum energy regeneration efficiency is obtained at a fixed electrical impedance coefficient. Following this section, it will be shown that the best net impedance coefficient for swing phase control may limit the maximum energy regeneration efficiency obtained. Fourth, the differences and similarities between the optimal and nonoptimal regulators will be discussed in each of three distinct cases. Finally, a block diagram of the optimal impedance regulator will be shown and discussed.

Before starting the derivations in this chapter, some definitions must be clarified. First of all, the net impedance coefficient (b_n), is defined as the total system "mechanical" viscous damping coefficient and is composed of the following two components: the mechanical impedance coefficient (b_m) which represents all the mechanical viscous damping in the knee system caused by friction, and the electrical impedance coefficient (b_e) which represents the

"mechanical" viscous damping in the system due to the electrical interaction with the generator. These relations are expressed by equation (4-1) below:

$$b_n = b_m + b_e. \qquad (4\text{-}1)$$

An net impedance coefficient will be selected for best swing phase control, so it is necessary to optimize the regeneration efficiency at a given b_n. Optimal energy regeneration efficiency will be found to be a function of b_e when b_n is held fixed.

To derive the regeneration efficiency, the equations for input and output power are first obtained.

The power into the knee system is equal to the knee torque times the angular velocity of the leg. (Coulombic friction is ignored in the following derivations.)

$$P_{IN} = T_n w = b_n w^2. \qquad (4\text{-}2)$$

The regenerated power (P_{OUT}) is stored in the capacitor. The time-averaged amount of power recovered by the capacitor, ignoring the AC component, is simply:

$$P_{OUT} = E_C i(1 - DC). \qquad (4\text{-}3)$$

where E_C, i, and DC are the capacitor voltage, motor current, and duty cycle respectively. The fraction of the time the motor current flows through the capacitor is equal to 1-DC.

The motor current can also be written in terms of the motor torque constant and b_e, as follows:

$$i = \frac{wb_e}{K_T}. \qquad (4\text{-}4)$$

Equation (3-5) is rewritten as equation (4-5) for convenience, but with the diode voltage drop E_D neglected.

$$i = \frac{wK_E - E_C(1 - DC)}{(R_F + R_M)}. \qquad (4\text{-}5)$$

Next, the motor current is eliminated by combining equations (4-4) and (4-5). The resulting equation is solved for 1-DC for later use.

$$\frac{wb_e}{K_T} = \frac{wK_E - E_C(1 - DC)}{(R_F + R_M)}. \qquad (4\text{-}6)$$

$$(1 - DC) = \frac{-wb_e(R_F + R_M)}{K_T E_C} + \frac{wK_E}{E_C}. \qquad (4\text{-}7)$$

Equation (4-8) is the result of substituting the right-hand side of equation (4-4) for the motor current, and the right-hand side of equation (4-7) for 1-DC, in equation (4-3). The fact that the motor torque constant, K_T, is equal to the motor voltage constant, K_E, of a permanent-magnet DC motor, is also used in the derivation of equation (4-8).

$$P_{OUT} = \frac{-w^2 b_e^2 (R_F + R_M)}{K_E^2} + w^2 b_e. \qquad (4\text{-}8)$$

The instantaneous efficiency of the knee system is equal to the power out divided by the power in. Dividing the right-hand side of equation (4-8) by the right-hand side of equation (4-2), the following is obtained:

$$\text{eff.} = \frac{P_{OUT}}{P_{IN}} = \frac{-(b_n - b_m)^2 (R_F + R_M)}{K_E^2 b_n} + \frac{b_n - b_m}{b_n}. \qquad (4\text{-}9)$$

To determine which b_e maximizes the efficiency of regeneration, the partial derivative of eff. with respect to b_e, is evaluated and set equal to zero.

$$\frac{deff.}{db_e} = \frac{-2b_e(R_F + R_M)}{K_E^2 b_n} + \frac{1}{b_n} = 0. \qquad (4\text{-}10)$$

This equation is then solved for b_e, obtaining a relation for the optimal b_e ($b_{e(OPT)}$) for energy regeneration:

$$b_{e(OPT)} = \frac{K_E^2}{2(R_F + R_M)}. \qquad (4\text{-}11)$$

Thus, given b_n for best swing phase performance, it is desirable to operate the generator at the optimal electrical impedance coefficient given by equation (4-11). It is also helpful to derive an expression for the maximum power out and for the efficiency penalty for not operating the generator at the optimal electrical impedance coefficient.

In order to compute the power out, the right-hand side of equation (4-11) is substituted into equation (4-8), and after rearrangement, the following is obtained:

$$P_{OUT(MAX)} = \frac{w^2 K_E^2}{4(R_F + R_M)}. \qquad (4\text{-}12)$$

This equation shows that the maximum amount of time-averaged power flowing into the capacitor is a function of the knee angular velocity squared.

Finally, the desired relation between b_e and the percentage of optimal energy regeneration (POER) at a given

b_n is found, after equations 4-8 and 4-12 are combined, to be:

$$\frac{POER.}{100} = \frac{P_{OUT}}{P_{OUT(OPT)}} = \frac{4b_e(R_F + R_M)\{K_E^2 - b_e(R_F + R_M)\}}{K_E^4}. \quad (4\text{-}13)$$

A plot of this equation is shown in Figure 4-1. Note that the largest amount of energy regeneration is always obtained at $b_{e(OPT)}$, and is independent of the capacitor voltage or knee angular velocity! However, as shown below, this optimal b_e is not always achievable. Nonetheless, the equations derived above will be used to develop an optimally-regenerative, impedance regulator.

The second goal of this chapter is to find an equation relating b_n to the regeneration efficiency of the knee system. If b_e is chosen as in the nonoptimal impedance regulator ($b_e=b_n-b_m$) or as in the optimal impedance regulator (a discussion on how b_e should be chosen will be given below), it is desirable compute which value of b_n will maximize the efficiency of the entire system. It is helpful to first define a constant as follows:

$$M = \frac{(R_F + R_M)}{K_E^2}. \quad (4\text{-}14)$$

Then, the partial derivative of efficiency with respect to b_n is taken and set equal to zero. Equation (4-1) is solved for b_e and substituted into equation (4-9). Equation (4-14) is used to simplify the resulting expression.

$$\frac{deff.}{db_n} = \frac{(1-2M(b_n - b_m))}{b_n} + \frac{M(b_n - b_m)^2 - (b_n - b_m)}{b_n^2} = 0. \quad (4\text{-}15)$$

Figure 4-1
PERCENTAGE OF OPTIMAL EFFICIENCY AS A
FUNCTION OF ELECT. IMPEDANCE COEFFICIENT
AT FIXED bn. [be(opt) = 2.12 N-M-Sec]

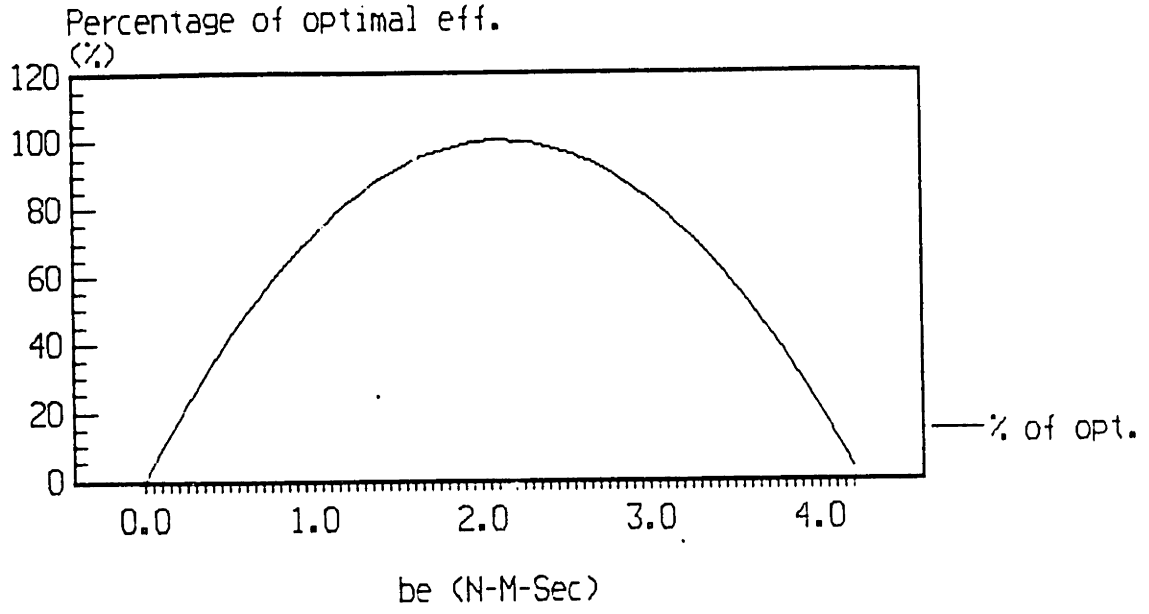

Figure 4-2
ENERGY REGENERATION EFFICIENCIES AS A
FUNCTION OF NET IMPEDANCE COEFFICIENT
[bn(opt) = 1.74 N-M-Sec]

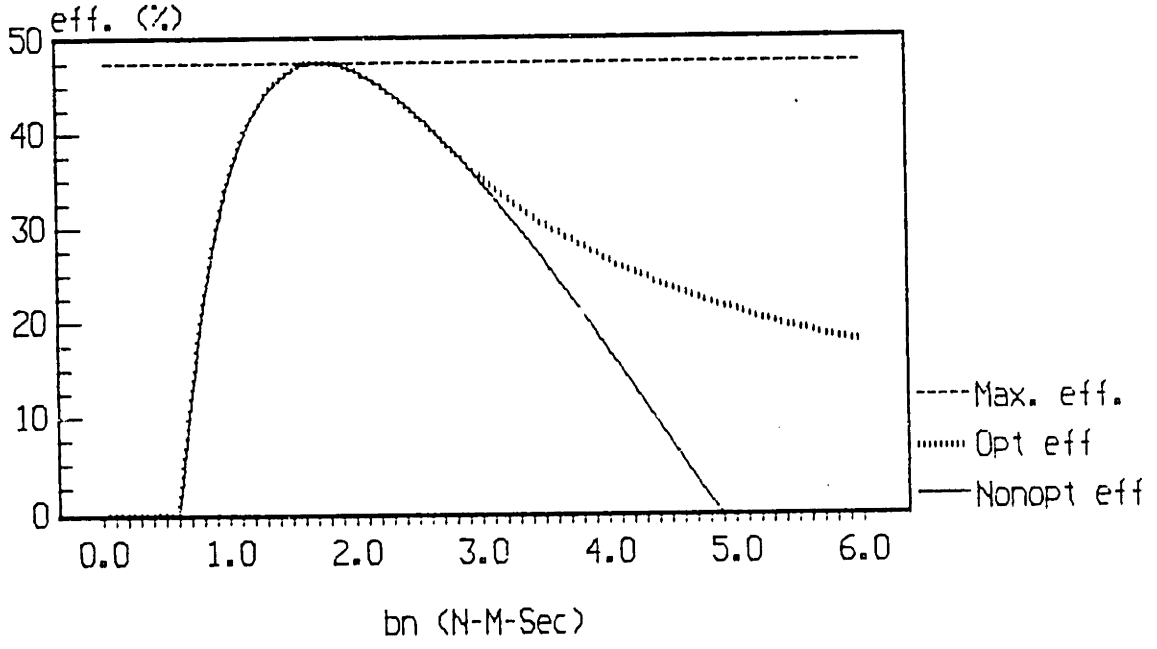

After rearrangement, the optimal net impedance coefficient is found to be as follows:

$$b_{n(OPT)} = \frac{(Mb_m^2 + b_m)^{1/2}}{M^{1/2}}. \qquad (4\text{-}16)$$

Therefore, the net impedance given by equation (4-16) can be the most energy efficient but not necessarily the most desirable from a control standpoint. Figure 4-2 shows that the most energy efficient b_n for the knee system ($b_{n(OPT)}$) is about 1.74 N-M-Sec independent of the impedance regulator type. To compute the plots shown, the most efficient b_e was used in each case. The particle brake impedance coefficient was zero for the nonoptimal regulator and the most desirable value for the optimal regulator.

The minimal achievable b_e is a function of capacitor voltage and angular velocity (see Figures 3-7 and 3-8), and the energy regeneration efficiency is a function of b_e, so it follows that the maximum efficiency is also a function of capacitor voltage and angular velocity as shown in Figures 4-3 and 4-4. Low capacitor voltages tend to reduce not only the controllability of the system but also the maximum achievable efficiency. Once again, high angular velocities and low capacitor voltages represent the worst case. It should be noted that these figures were derived only for the nonoptimal regulator. The differences between the regulators will be discussed in the next section.

The nonoptimal impedance regulator design of the previous chapter can easily be modified to include optimal

Figure 4-3
MAXIMUM ENERGY REGENERATION EFFICIENCY
AS A FUNCTION OF ANGULAR VELOCITY AND
CAPACITOR VOLTAGE

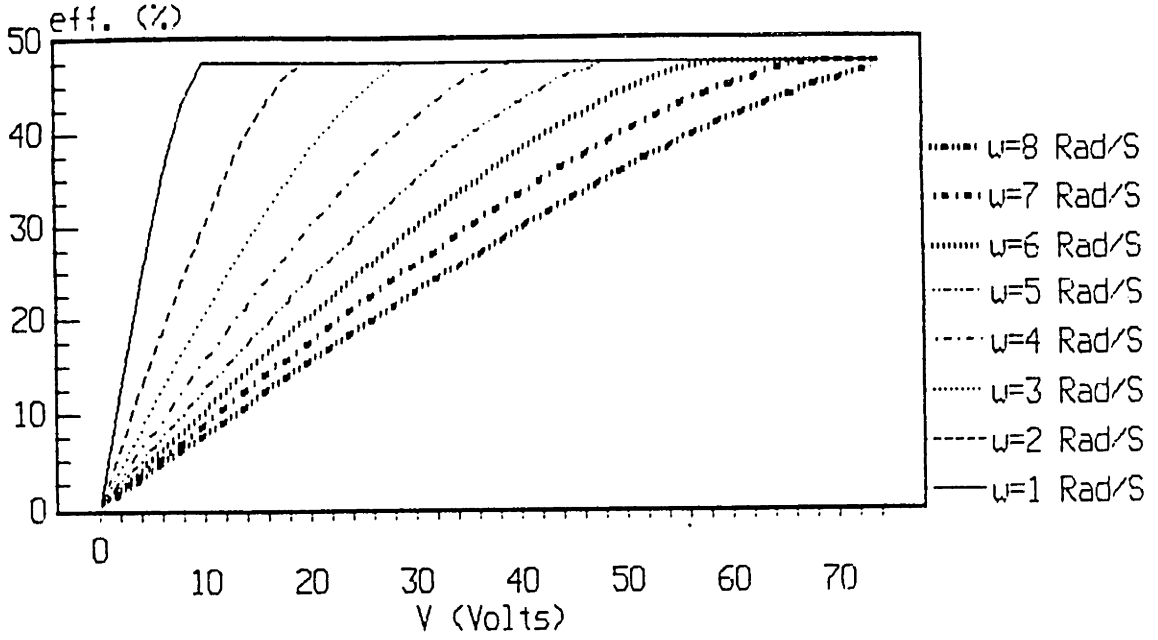

Figure 4-4
MAXIMUM ENERGY REGENERATION EFFICIENCY
AS A FUNCTION OF CAPACITOR VOLTAGE AND
ANGULAR VELOCITY

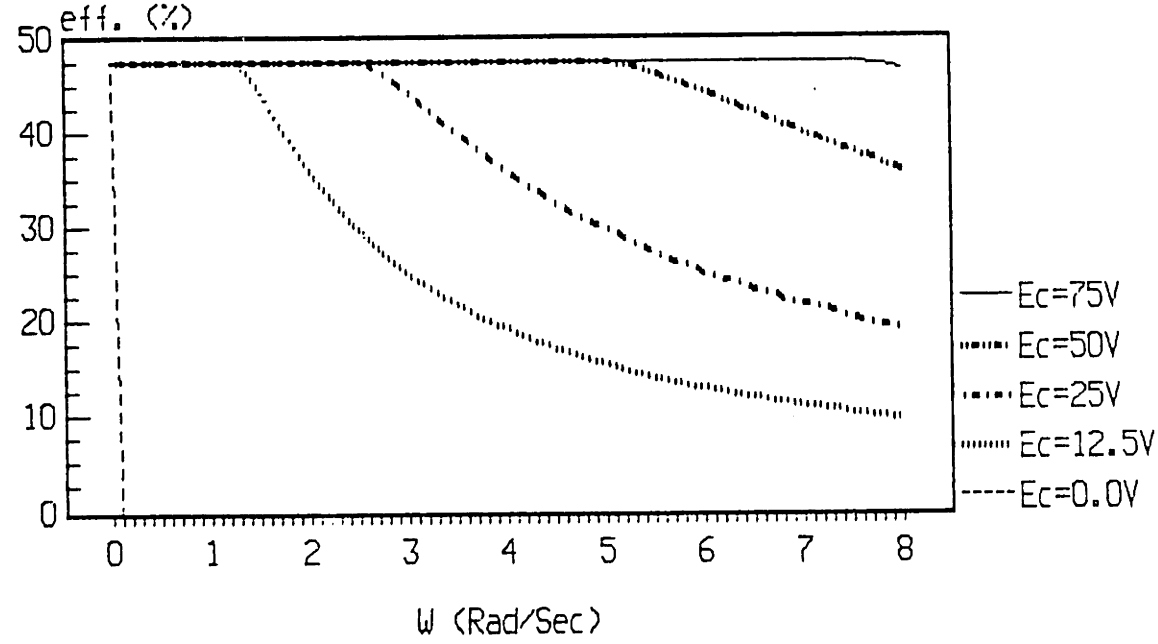

energy regeneration. To illustrate this, three distinct cases must be examined: one when b_n-b_m is less than or equal to $b_{e(OPT)}$, one when b_n-b_m is greater than $b_{e(OPT)}$, and one during low capacitor voltages. In the first two cases, it is assumed that b_n is chosen as a compromise between good swing phase control and good energy efficiency and that the electrical and brake impedance coefficients remain to be determined in order to achieve optimal efficiency. The three case will be described in detail below.

First, if b_n-b_m is less than or equal to $b_{e(OPT)}$, then the nonoptimal impedance regulator is already operating at maximum efficiency at the given b_n. The magnetic-particle brake is not needed from a regeneration standpoint (ie. the brake impedance, b_b, is zero). However, note that a trade-off between energy regeneration efficiency and desired gait performance may exist in this case. A larger b_n, and hence, b_e, than necessary for best swing phase control, may increase energy efficiency, but will result in less desirable gait.

Second, if the b_n-b_m is greater than $b_{e(OPT)}$, then the magnetic-particle brake can be used to develop a portion of the impedance (b_b=b_n-b_m-$b_{e(OPT)}$), such that the generator still develops $b_{e(OPT)}$. This is the only case when the optimal and nonoptimal impedance regulators will differ, except when the capacitor is discharged.

Third, when the capacitor voltage is low, a large duty cycle change has almost no effect on control but does affect

regeneration. In this case, the duty cycle should always be set to zero for two reasons. First, energy will be recovered in the capacitor and, second, the capacitor voltage will increase--resulting in a more controllable and efficient knee.

An optimally-regenerative impedance regulator design results when the nonoptimal impedance regulator design of the previous chapter is modified according to the three cases discussed above. The changes to the original regulator are relatively small. A block diagram of the optimally-regenerative impedance regulator is shown in Figure 4-5. However, two things in particular are worth noting. In the present system, with the magnetic-particle brake always mechanically connected, the particle brake may dissipate an appreciable amount of energy when not in use, so that it may be better not to use the brake at all from an energy standpoint. Second, note the somewhat counterintuitive result--a generator/particle brake combination is sometimes more efficient than a generator alone.

In summary, it has been demonstrated that the optimum b_n for swing phase control may not be the optimum b_n for energy efficiency. Therefore, a compromise must be made in the selection of b_n. However, once b_n is chosen, it was shown how to select b_e and b_b to maximize efficiency. The last section described how the optimal and nonoptimal impedance regulators differ.

FIGURE 4-5: OPTIMAL IMPEDANCE REGULATOR BLOCK DIAGRAM

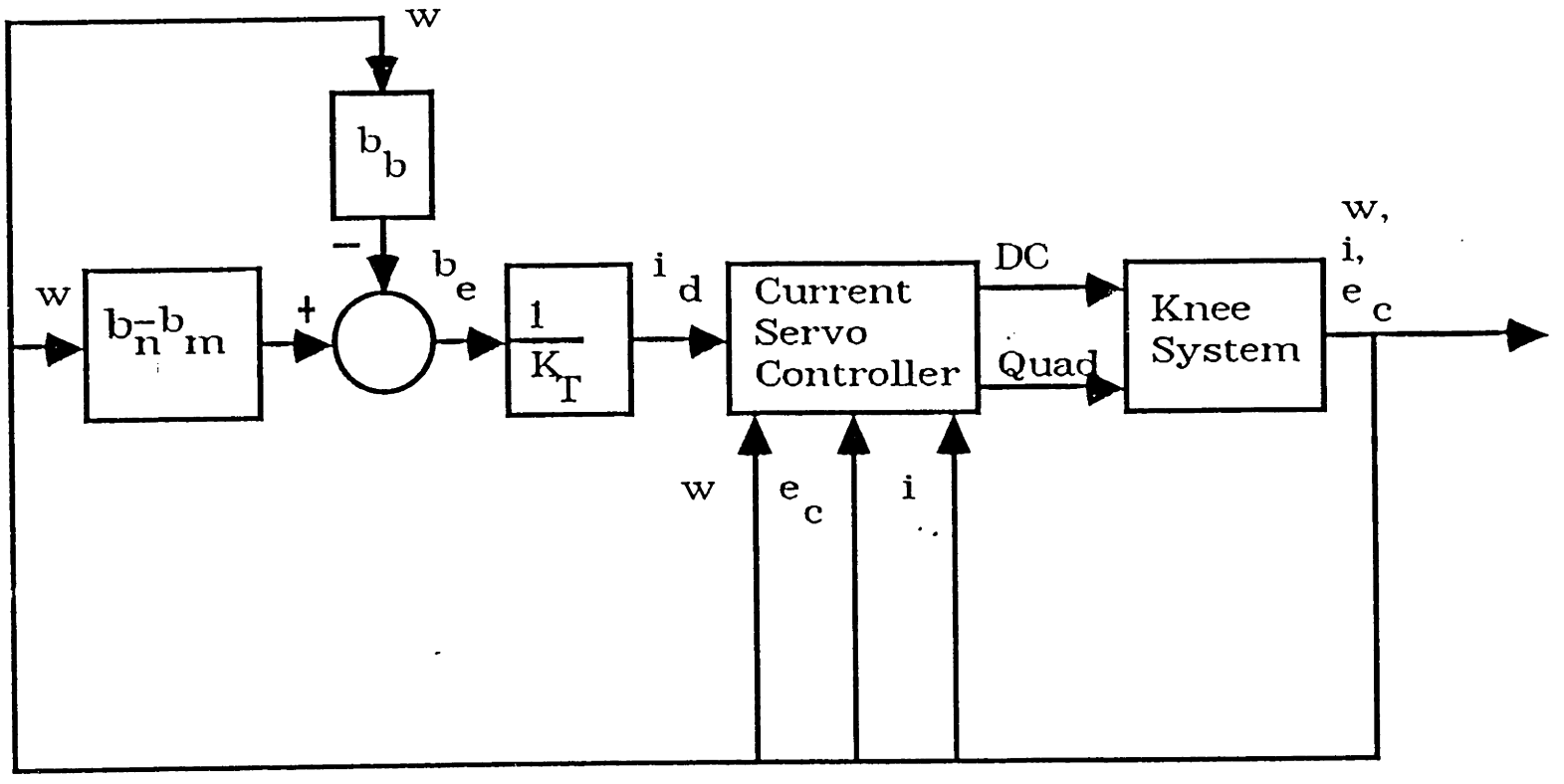

NOTE: If bn-bm < be(opt) then be=bn-bm and bb=0,
else be=be(opt) and bb=bn-bm-be(opt).

In the next chapter, experimental results will be presented that will verify the operation of the nonoptimal impedance regulator. The unavoidably large impedance at low capacitor voltages will also be shown to be independent of duty cycle as predicted in chapter three.

Chapter Five

Experimental Results

In this chapter, experimental results will show that the nonoptimal impedance regulator functioned as explained in the previous chapters. In particular, it will be shown that four different levels of electrical impedance could be obtained. The response associated with a step change in desired electrical impedance coefficient (b_e) will demonstrate the dynamic response of the controller. Next, some of the remaining problems of the regulator will be explained mostly with experimental data. Finally, the regeneration efficiency of the regulator at various electrical impedance coefficients will be displayed.

First of all, to obtain acceptable gait, the impedance regulator must control the electrical impedance or rotational viscous damping coefficient. Under many operating conditions, it is possible to obtain the desired b_e nearly exactly. The operation of the regulator with four different b_e is shown in Figures 5-1 through 5-4. However, before the figures are examined in detail some explanation is necessary.

Each figure (one trial) consists of four separate graphs. None of the data in these graphs were filtered off-line. Only the motor current and capacitor voltage were low-pass filtered in hardware before sampling. Each of four graphs per trial are explained below.

In each case, the first of the four graphs shows the desired duty cycle (Dsrd DC), the actual duty cycle (Act DC), and the knee angular velocity (w). The desired duty cycle was the duty cycle which was necessary, according to the model (equation (3-7)), to create the desired knee electrical impedance coefficient. The actual duty cycle was the duty cycle that the control program actually requested. The actual and desired duty cycles were nearly exactly the same--demonstrating that the regulator was requesting the proper duty cycle. The knee angular velocity was obtained by simply dividing the change in angular position by the time interval. The noise on the angular velocity curve was due to the quantization noise of the optical encoder. A data point for each of the curves was obtained every 4 mS (the control frequency was 250 Hz).

The second graph in each case shows the predicted current (Pred I) and the actual current (Act I). The predicted current was the current that was estimated by using the model of chapter three. The actual current was the current sampled by the computer after first being low-pass filtered in hardware.

The third graph in each case is a plot of the capacitor voltage (Ec). The signal was low-pass filtered in hardware.

The final graph in each trial shows the desired impedance (Dsrd b_e) and the actual impedance (Act b_e). The torque (T_e) was determined by multiplying the motor torque constant by the motor current (ie. $T_e=K_T i$). Note that the

Figure 5-1A
IMPEDANCE REGULATOR OPERATION-TRIAL I
Angular Velocity and Duty Cycles
Vs. Time

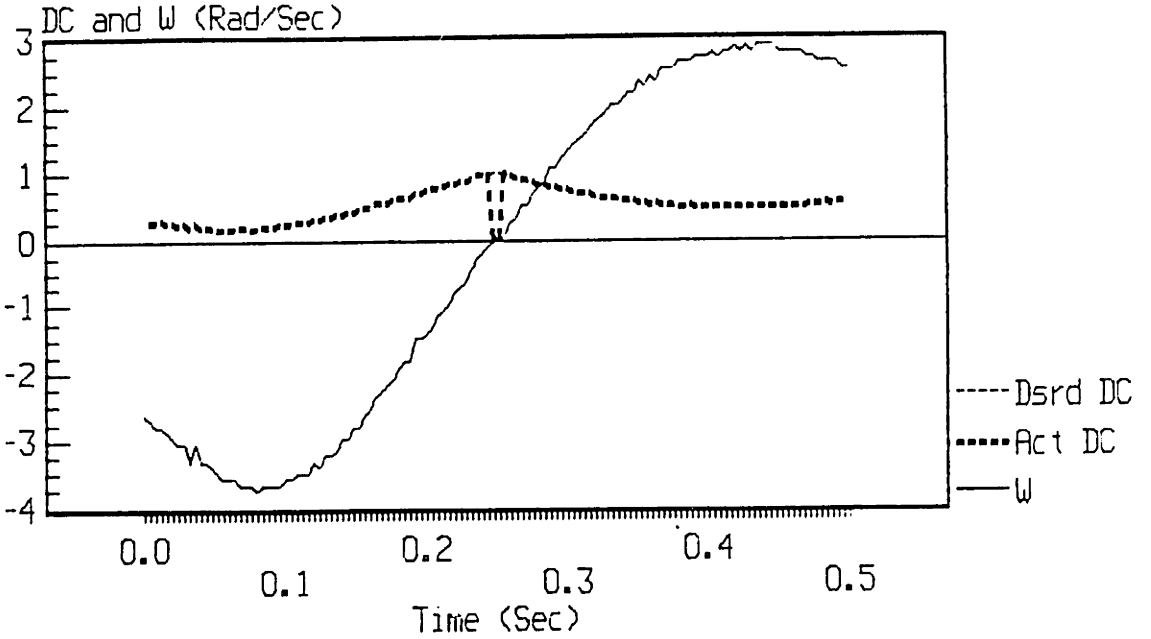

Figure 5-1B
IMPEDANCE REGULATOR OPERATION-TRIAL I
Predicted and Actual Current Vs. Time

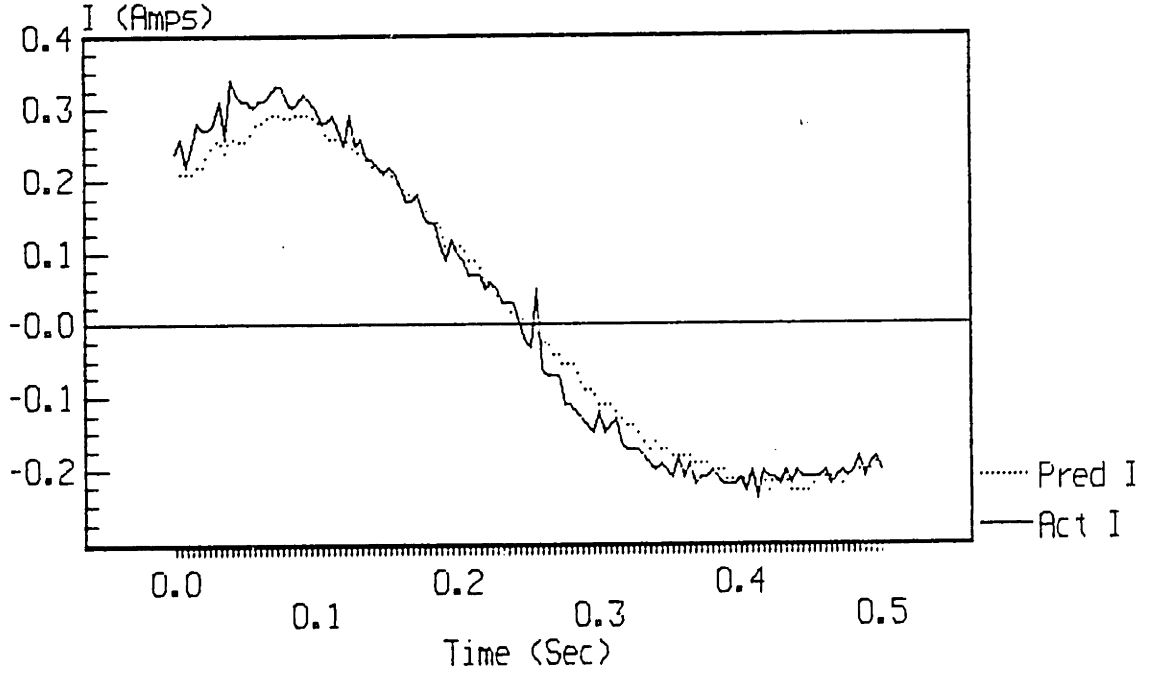

Figure 5-1C
IMPEDANCE REGULATOR OPERATION-TRIAL I
Capacitor Voltage Vs. Time

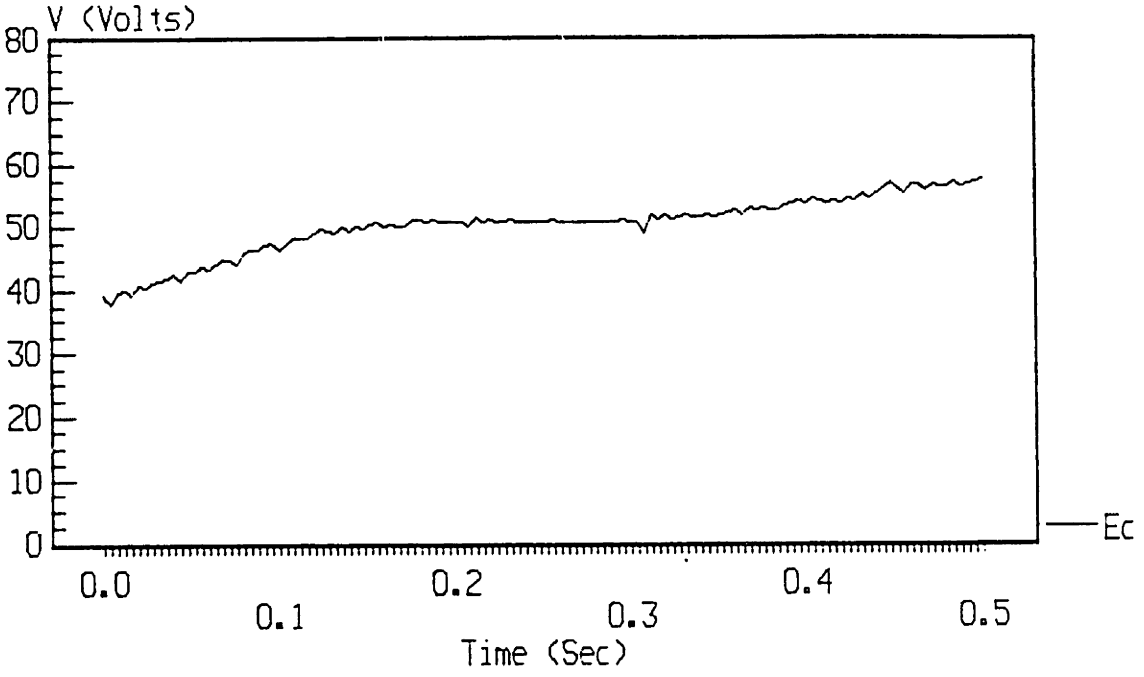

Figure 5-1D
IMPEDANCE REGULATOR OPERATION-TRIAL I
Desired and Actual Knee Impedance
Coefficients

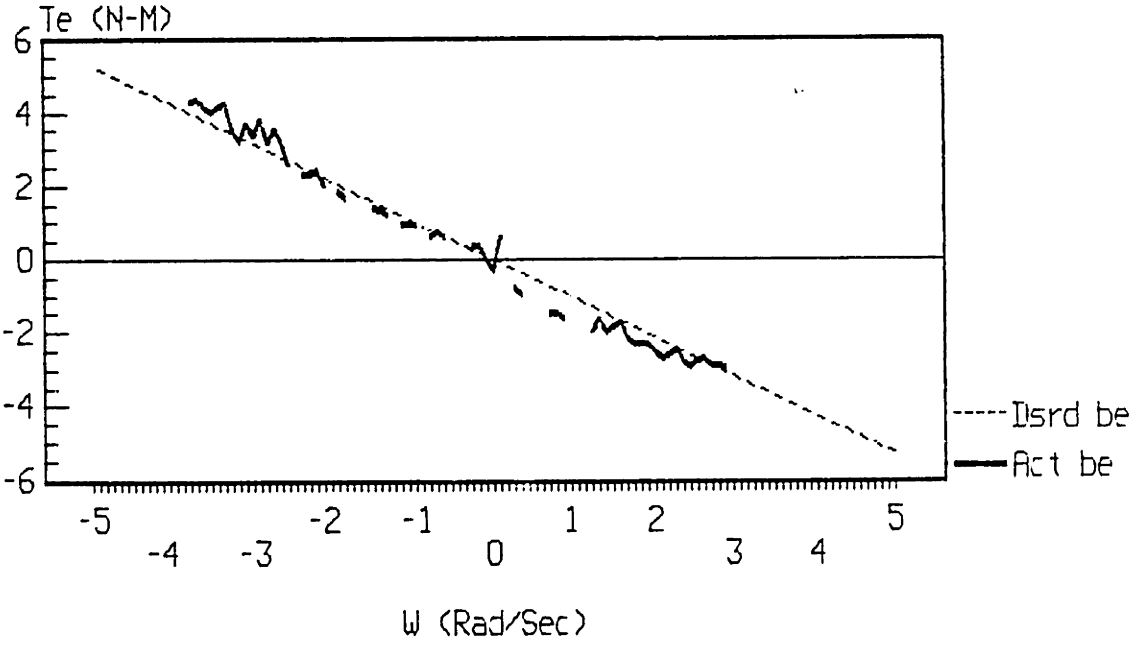

Figure 5-2A
IMPEDANCE REGULATOR OPERATION-TRIAL II
Angular Velocity and Duty Cycles
Vs. Time

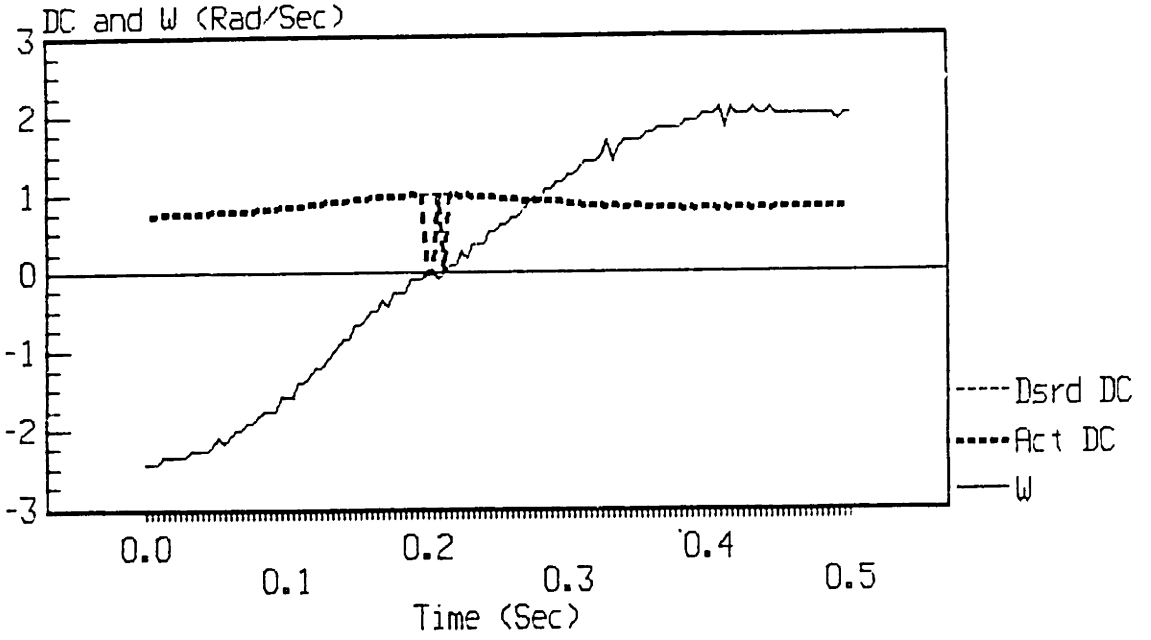

Figure 5-2B
IMPEDANCE REGULATOR OPERATION-TRIAL II
Predicted and Actual Current Vs. Time

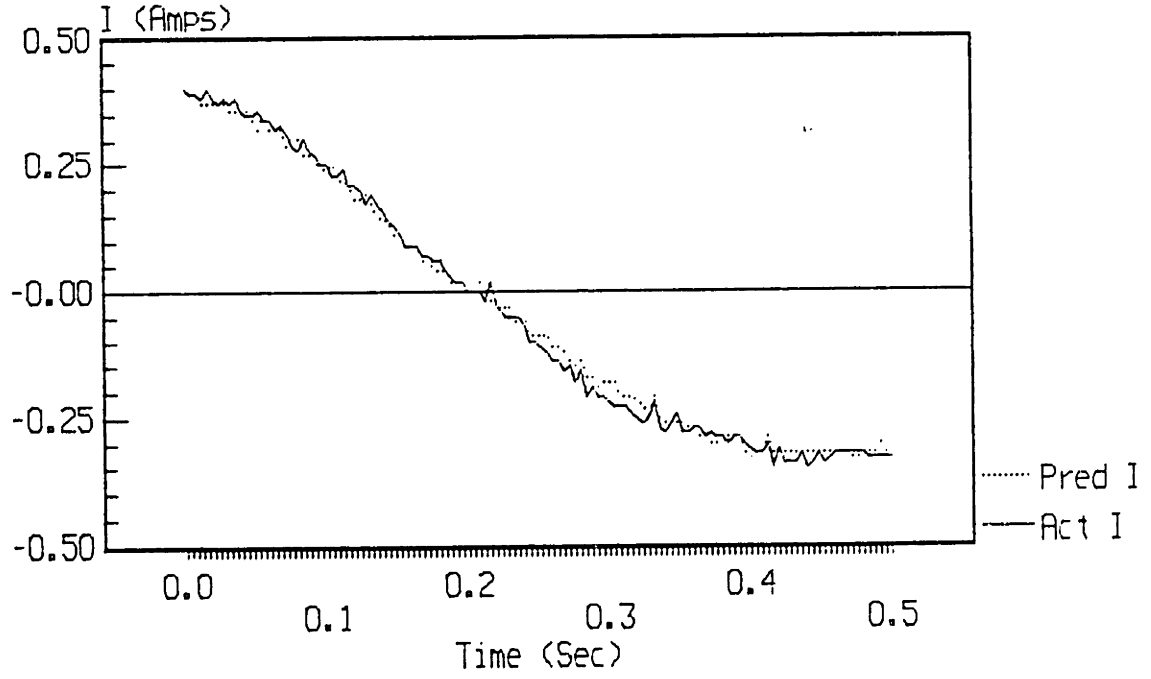

Figure 5-2C
IMPEDANCE REGULATOR OPERATION-TRIAL II
Capacitor Voltage Vs. Time

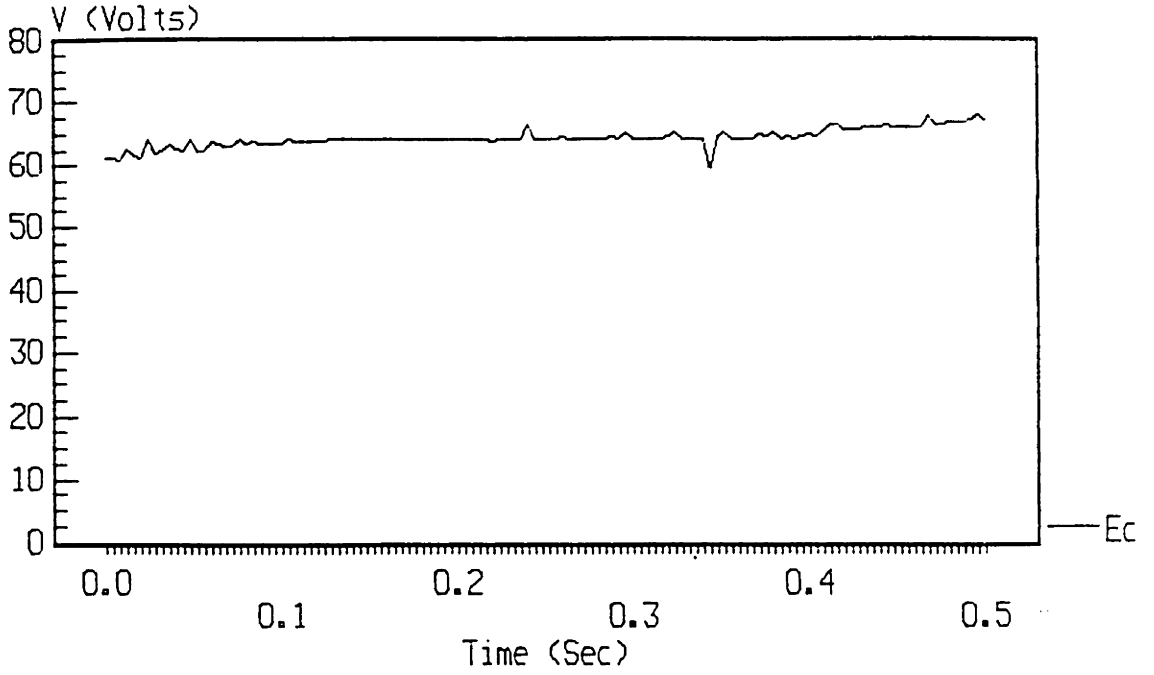

Figure 5-2D
IMPEDANCE REGULATOR OPERATION-TRIAL II
Desired and Actual Knee Impedance
Coefficients

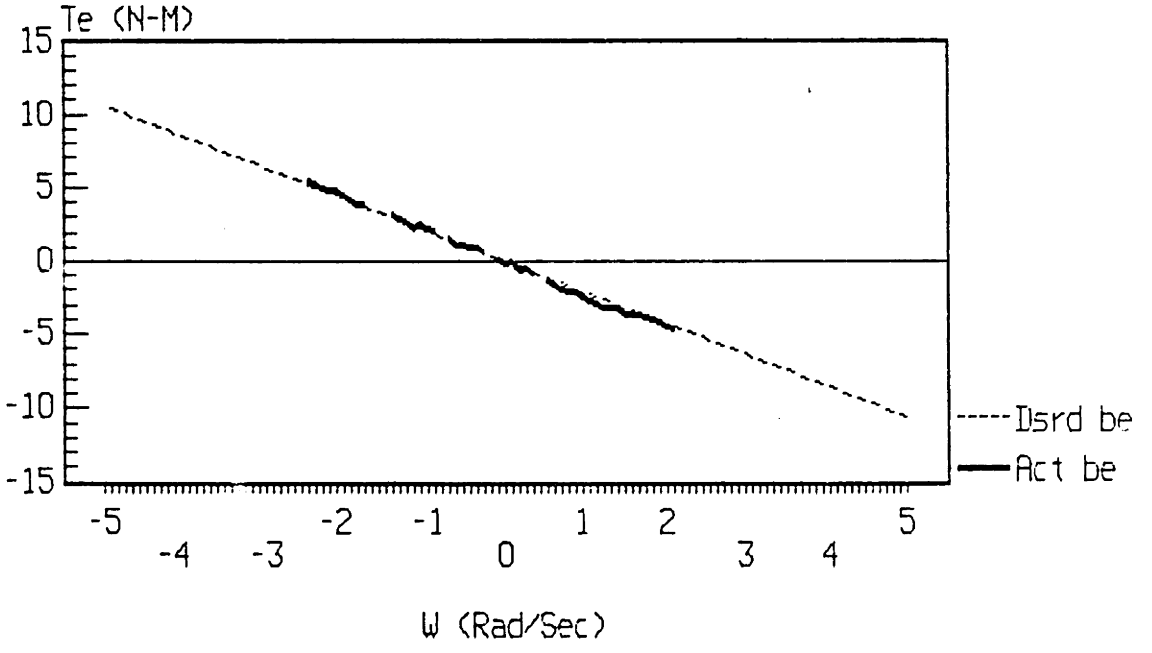

Figure 5-3A
IMPEDANCE REGULATOR OPERATION-TRIAL III
Angular Velocity and Duty Cycles
Vs. Time

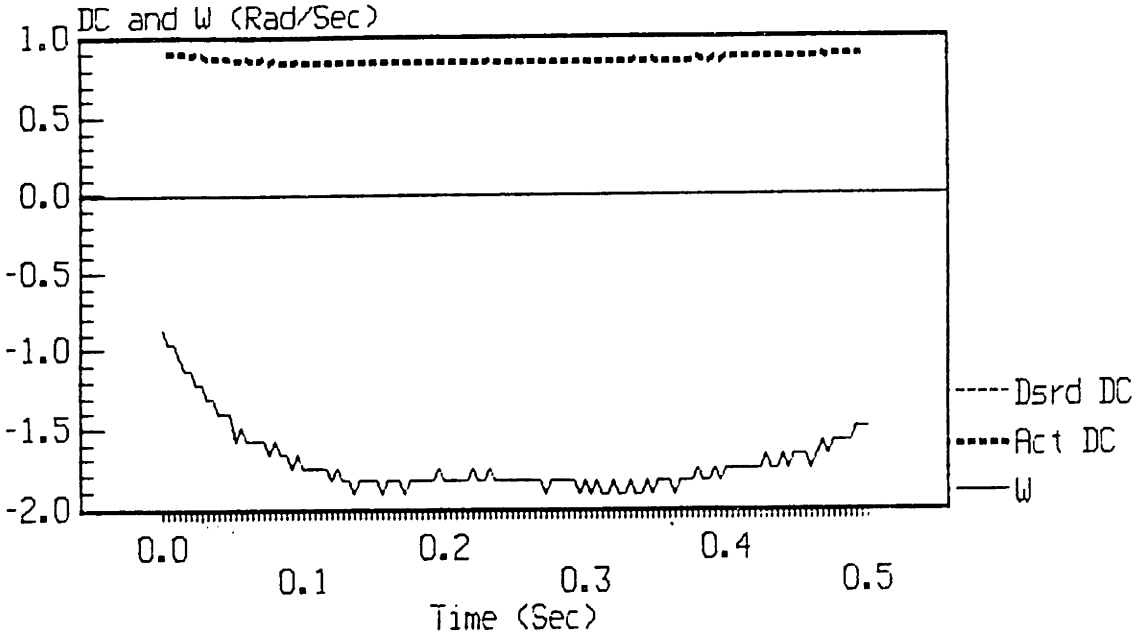

Figure 5-3B
IMPEDANCE REGULATOR OPERATION-TRIAL III
Predicted and Actual Current Vs. Time

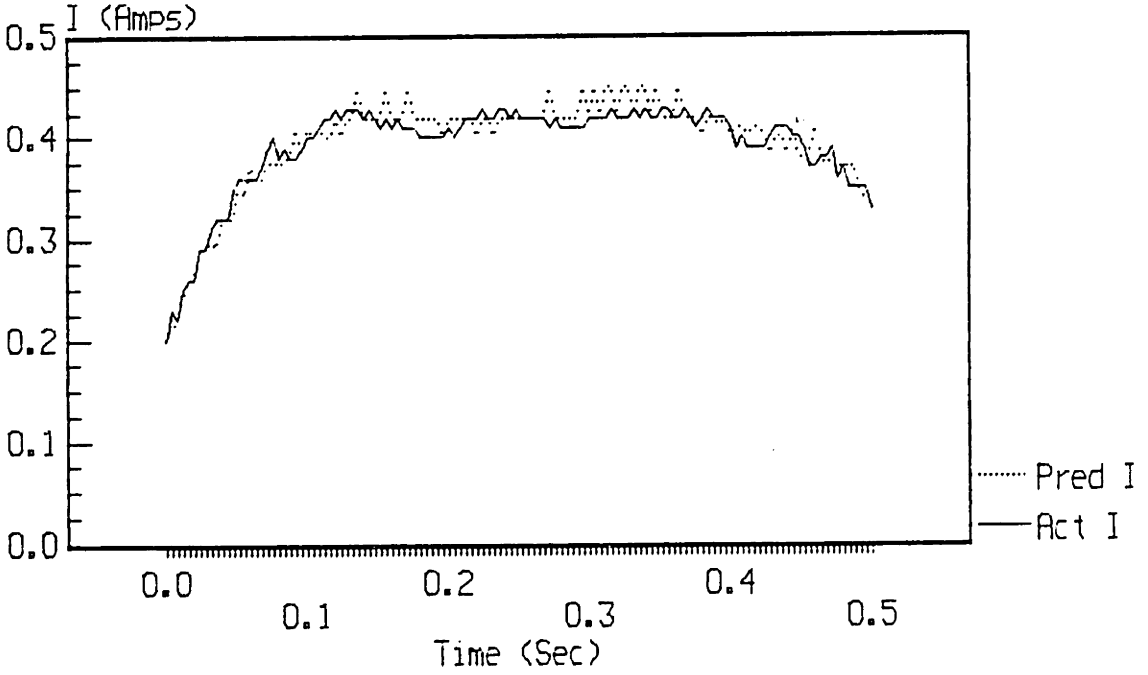

Figure 5-3C
IMPEDANCE REGULATOR OPERATION-TRIAL III
Capacitor Voltage Vs. Time

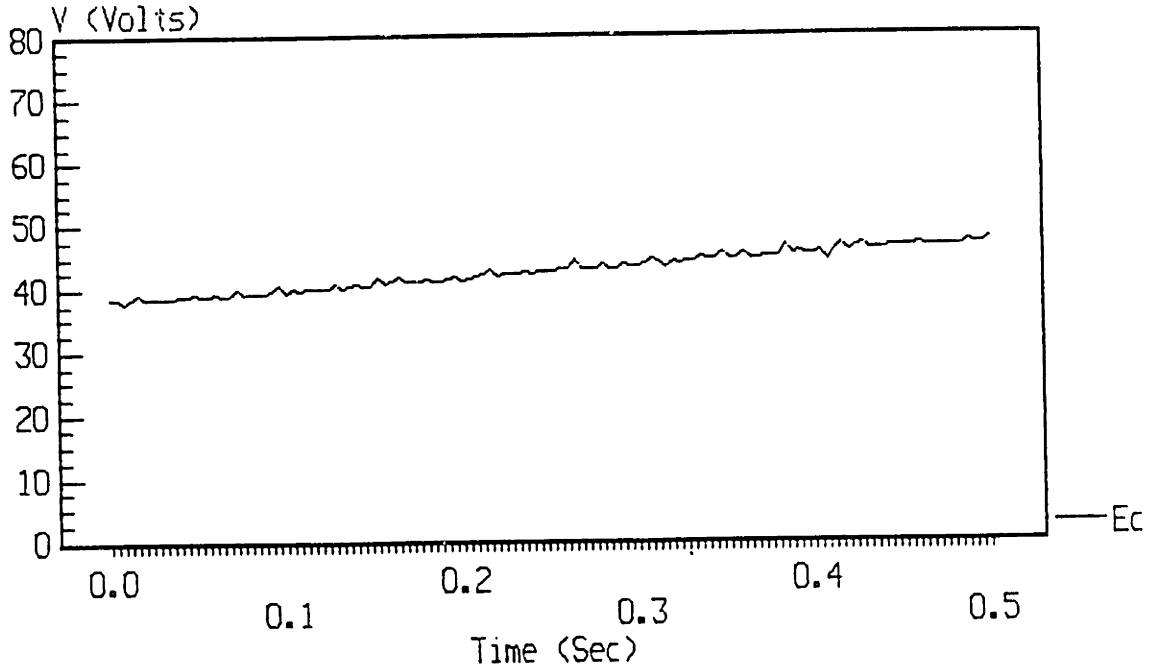

Figure 5-3D
IMPEDANCE REGULATOR OPERATION-TRIAL III
Desired and Actual Knee Impedance
Coefficients

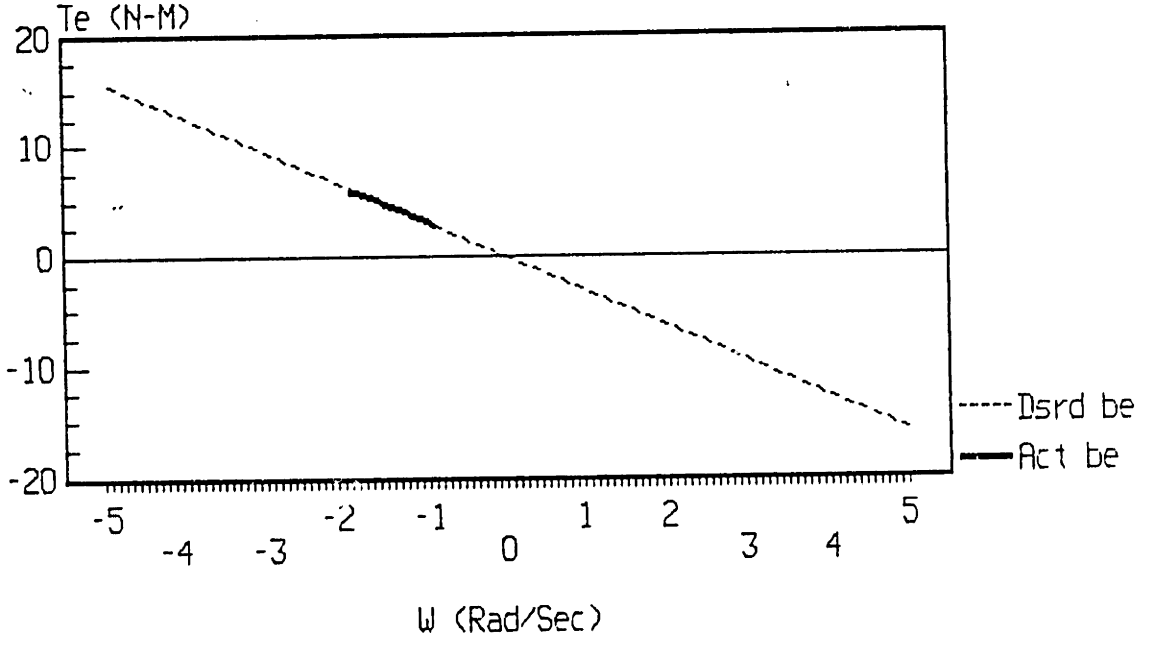

Figure 5-4A
IMPEDANCE REGULATOR OPERATION-TRIAL IV
Angular Velocity and Duty Cycles
Vs. Time

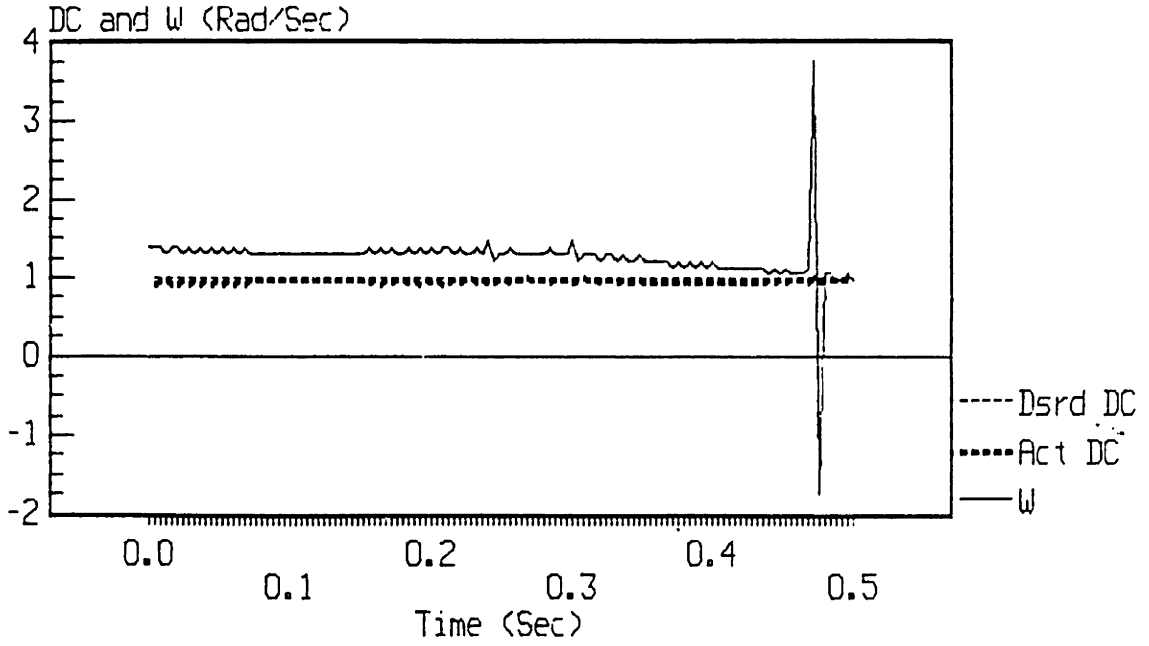

Figure 5-4B
IMPEDANCE REGULATOR OPERATION-TRIAL IV
Predicted and Actual Current Vs. Time

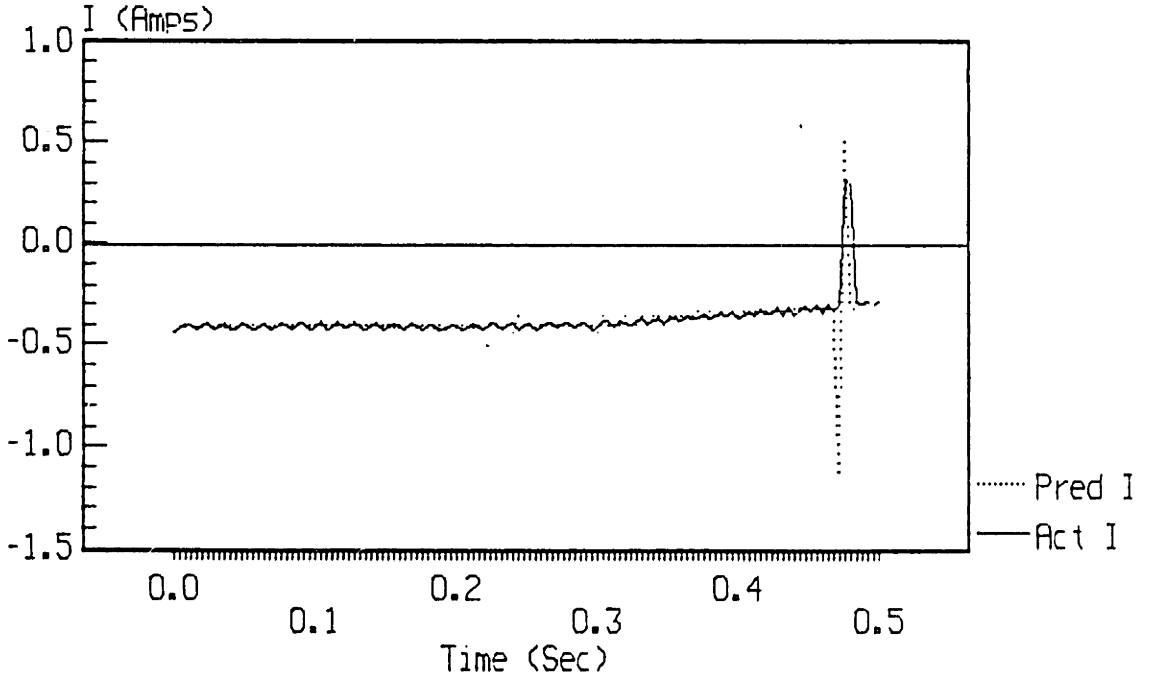

Figure 5-4C
IMPEDANCE REGULATOR OPERATION-TRIAL IV
Capacitor Voltage Vs. Time

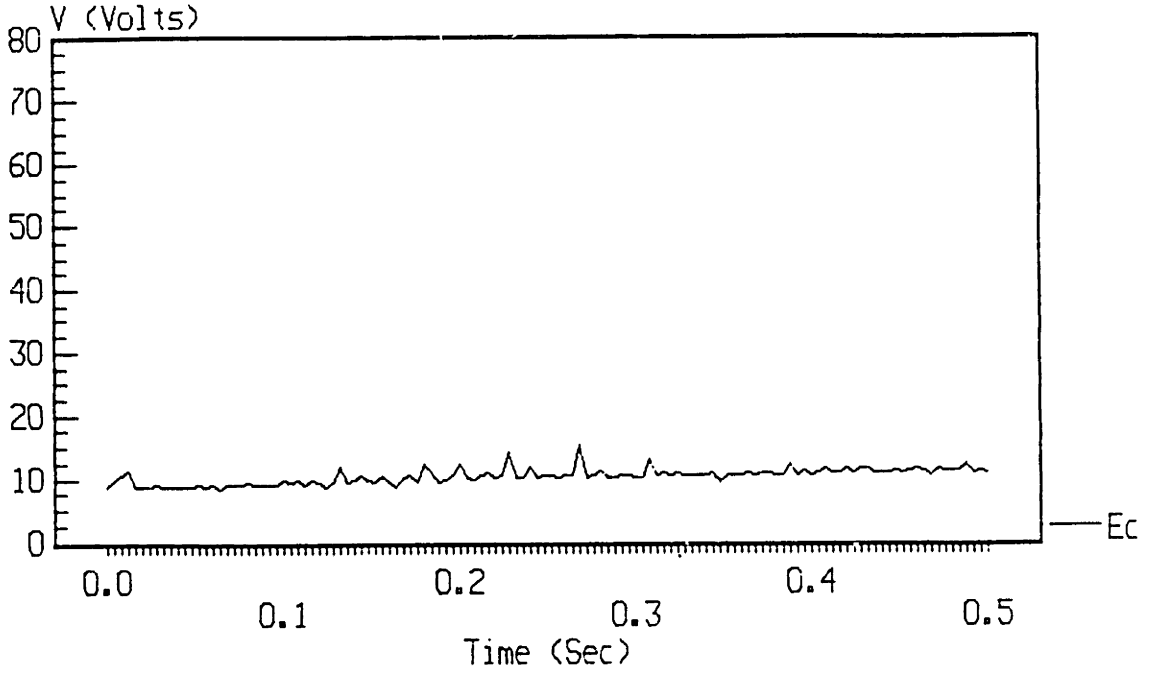

Figure 5-4D
IMPEDANCE REGULATOR OPERATION-TRIAL IV
Desired and Actual Knee Impedance
Coefficients

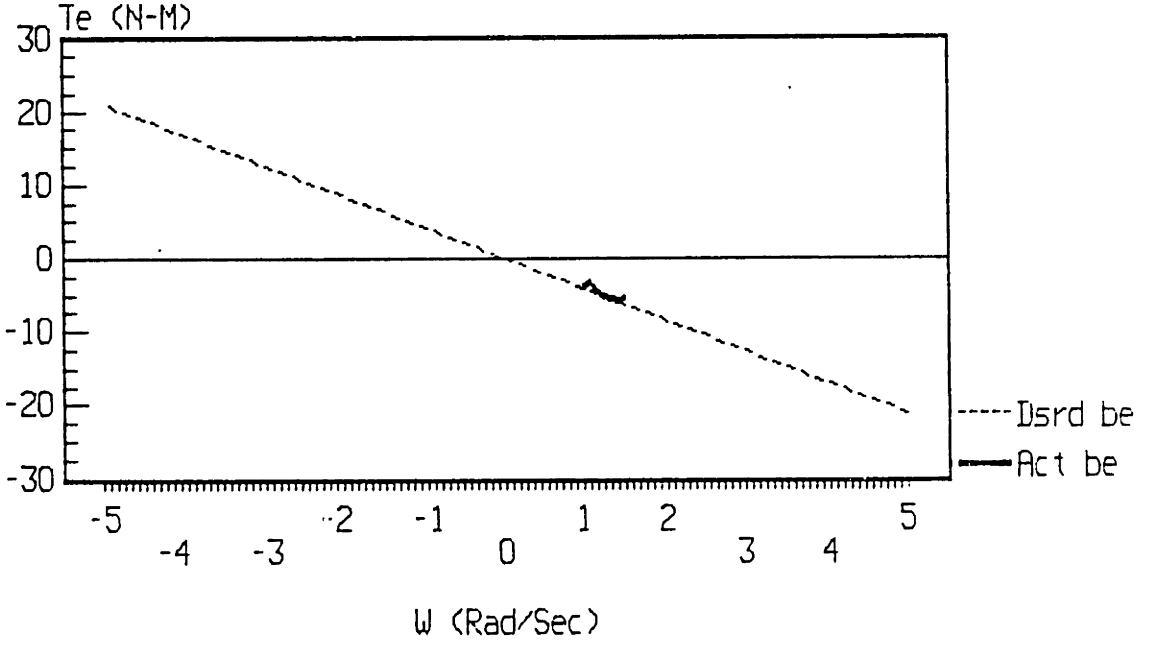

torque was directed in the opposite direction as the knee angular velocity because an opposing or viscous torque was desired. The actual b_e curve is not continuous since not all discrete velocities were recorded between the extremes. Also, it should be noted that the actual impedance values obtained are averages of the knee torques at a given discrete angular velocity.

An electrical impedance coefficient (b_e) of 1.06 N-M/Sec (25% of the maximum) was desired in the first trial. The knee was oscillated approximately sinusoidally. The plots in Figure 5-1 show that the capacitor voltage was increasing, indicating that energy regeneration was occurring. Also, the desired knee b_e was obtained almost exactly. The actual motor current lagged the predicted motor current due to the phase shift of the low-pass filter used (Figure 5-1B). The regulator worked quite nicely in this trial.

In the second trial, an electrical impedance coefficient twice as large as in the first trial, was desired (b_e=2.12 N-M/Sec, 50% of maximum). Figure 5-2A shows that the actual duty cycle went to zero when the angular velocity went to zero. This is the only known case where the actual and desired duty cycles differed significantly, and in this case the error was not important. Figure 5-2B shows that the predicted and actual motor current agreed almost exactly. Figure 5-2C shows that the capacitor was charging. The capacitor voltage increased

much slower in this trial since the energy stored in a capacitor is proportional to the voltage squared. Last of all, Figure 5-2D shows that the actual b_e and desired b_e were nearly identical.

In the third trail, a b_e of 3.18 N-M/Sec (75% of the maximum) was desired. The results show that the knee was always traveling in the negative direction. The predicted and actual current were nearly the same as shown in Figure 5-3B. Note that there was "noise" in the predicted motor current that was directly caused by quantization noise in the knee velocity. The capacitor was charging, indicating that energy was being recovered as shown in Figure 5-3C. In Figure 5-3D, it is evident that the desired and actual impedances were nearly identical.

Maximum electrical impedance was desired in the fourth trial (b_e=4.24 N-M/Sec). Maximum impedance means that the motor is always shorted and theoretically never connected to the capacitor. However, since the real duty cycle never exceeded about 95%, a small amount of energy was recovered as shown in Figure 5-4C.

A glitch in the knee velocity data is shown near the end of Figure 5-4A. Note that a glitch in the predicted and actual motor current resulted. During the experiments, glitches like this were actually felt but did not generally represent a serious problem. The glitches were caused by reading first the low and then the high byte of the digital position counter while it was changing--causing an error in

position and in velocity (velocity data were derived from the change in position). Nonetheless, the glitch did not create a noticeable time-averaged change in knee impedance.

In each of the four different trials discussed above, the desired and actual knee electrical impedance coefficients were nearly identical. Energy regeneration efficiency was not computed in these cases due to an unreliable knee torque signal. For this reason, the knee torque data was not presented in this work. Energy regeneration efficiency will, however, be investigated later in this chapter.

A step change in impedance illustrated the dynamic response of the impedance regulator. As shown in Figure 5-5, the response of the regulator to a step change in desired electrical impedance coefficient was nearly instantaneous. A fast response is highly desirable because it becomes possible to modulate the impedance coefficient as a function of position, direction, velocity, and any of a host of other variables. It allows the use of many other types of impedance control.

Four problems that can disrupt the nearly ideal operation of the regulator shown above still remain. Each of these problems will be discussed below but experimental data will not be used to confirm all of them.

In particular, the knee was both uncontrollable and inefficient at low capacitor voltages as explained in chapters three and four. This was the most serious problem

Figure 5-5A
IMPEDANCE REGULATOR DYNAMIC RESPONSE
Angular Velocity and Duty Cycles
Vs. Time

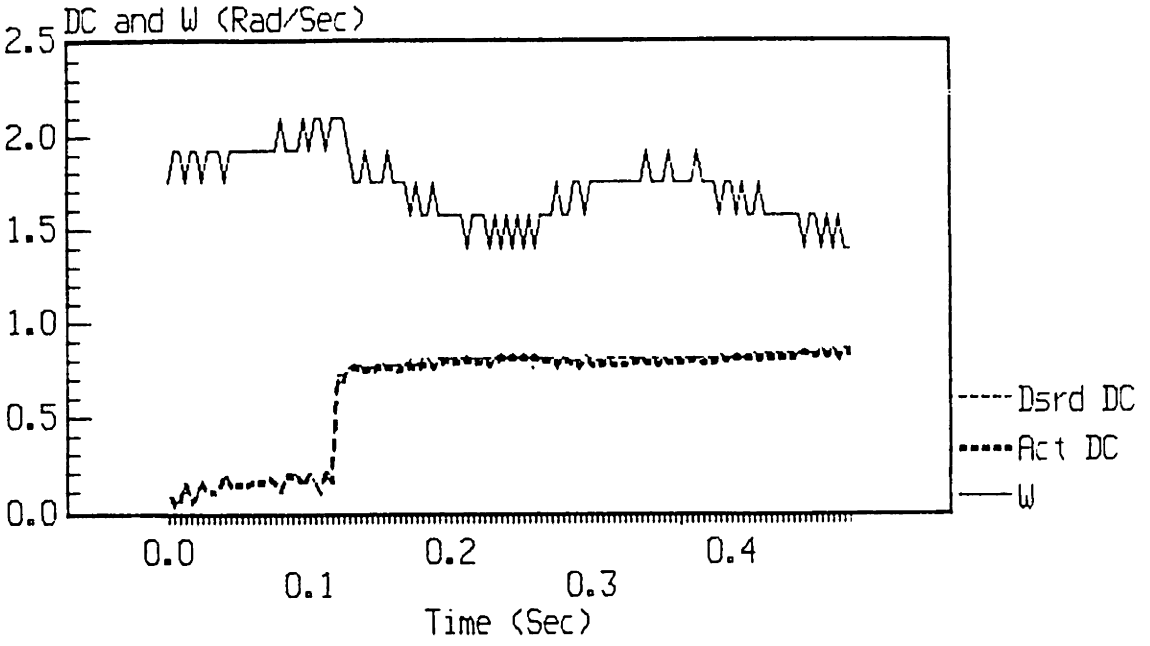

Figure 5-5B
IMPEDANCE REGULATOR DYNAMIC RESPONSE
Predicted and Actual Current Vs. Time

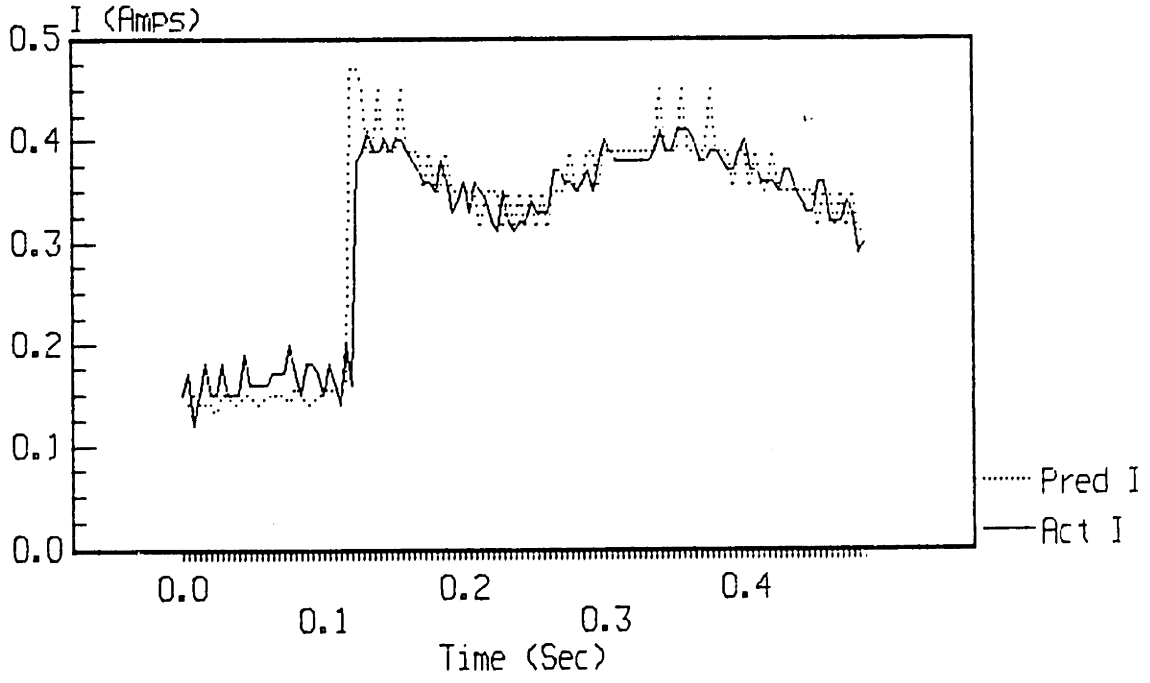

Figure 5-5C
IMPEDANCE REGULATOR DYNAMIC RESPONSE
Capacitor Voltage Vs. Time

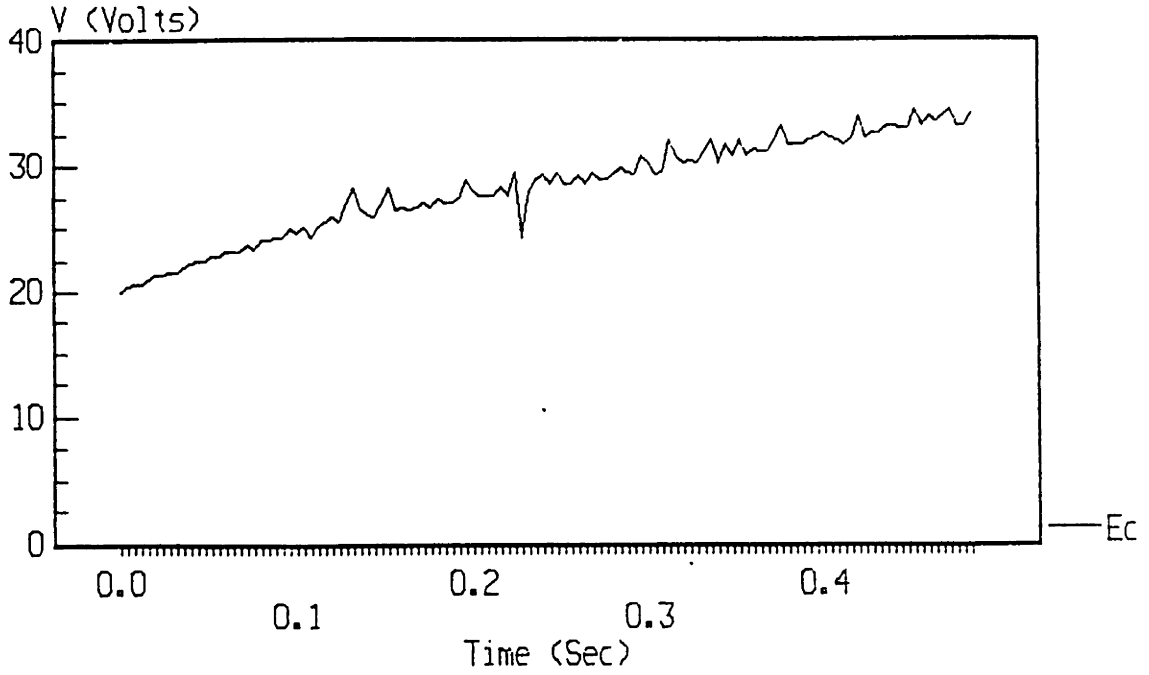

Figure 5-5D
IMPEDANCE REGULATOR DYNAMIC RESPONSE
Desired and Actual Knee Impedance
Coefficients

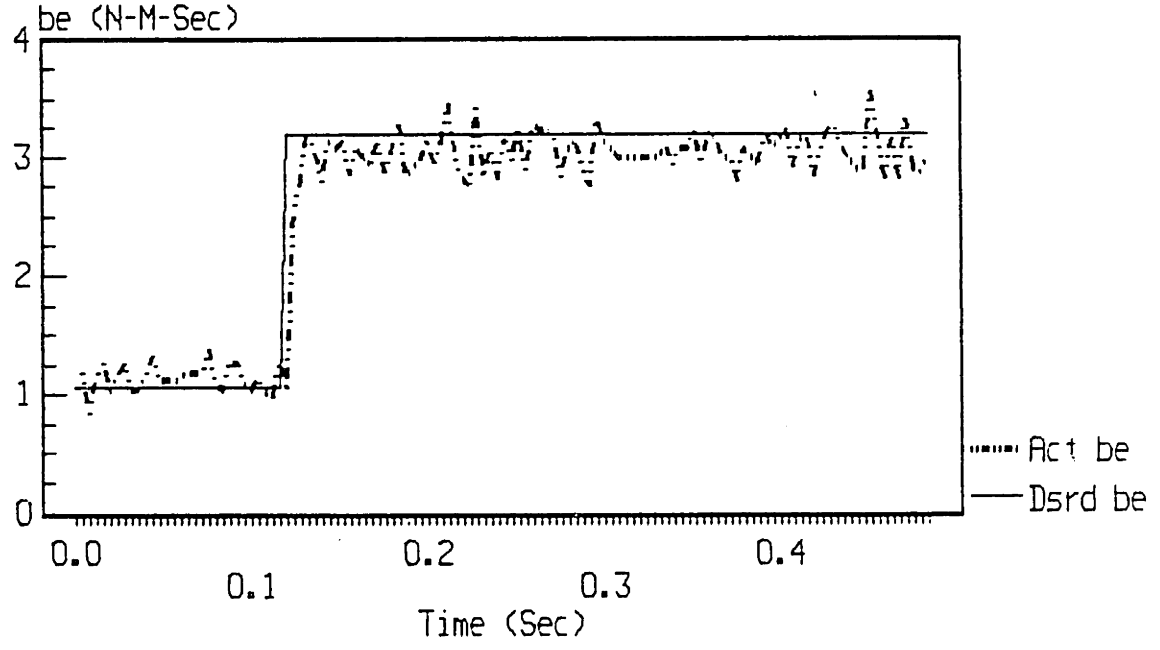

Figure 5-6A
IMPEDANCE REGULATOR UNCONTROLLABILITY
Angular Velcity and Duty Cycles
Vs. Time

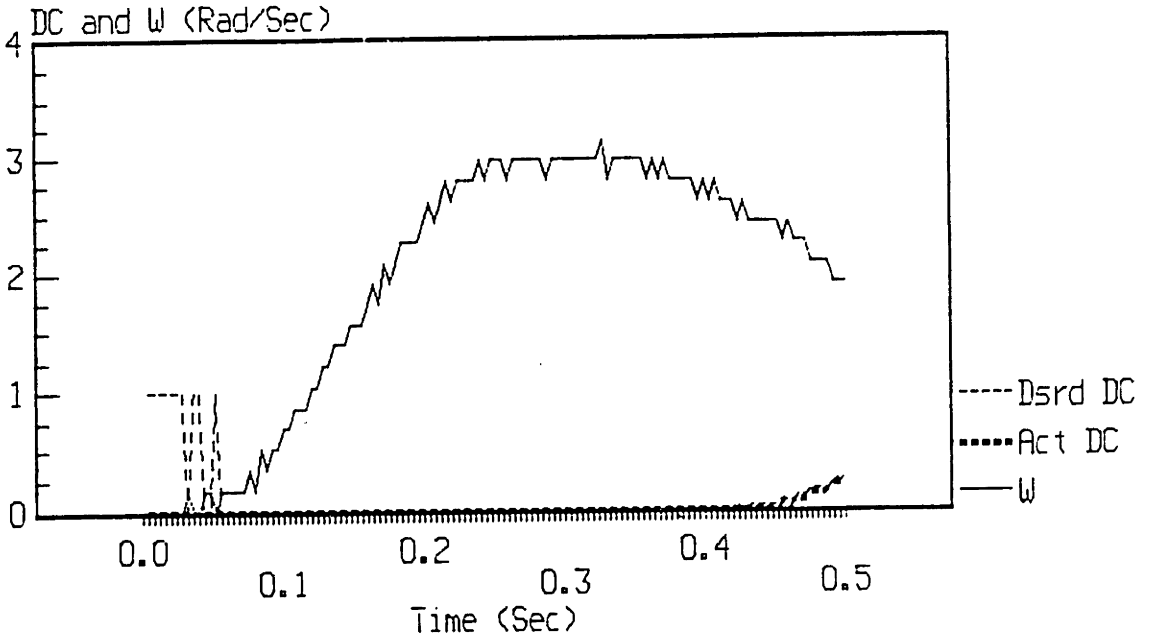

Figure 5-6B
IMPEDANCE REGULATOR UNCONTROLLABILITY
Predicted and Actual Current Vs. Time

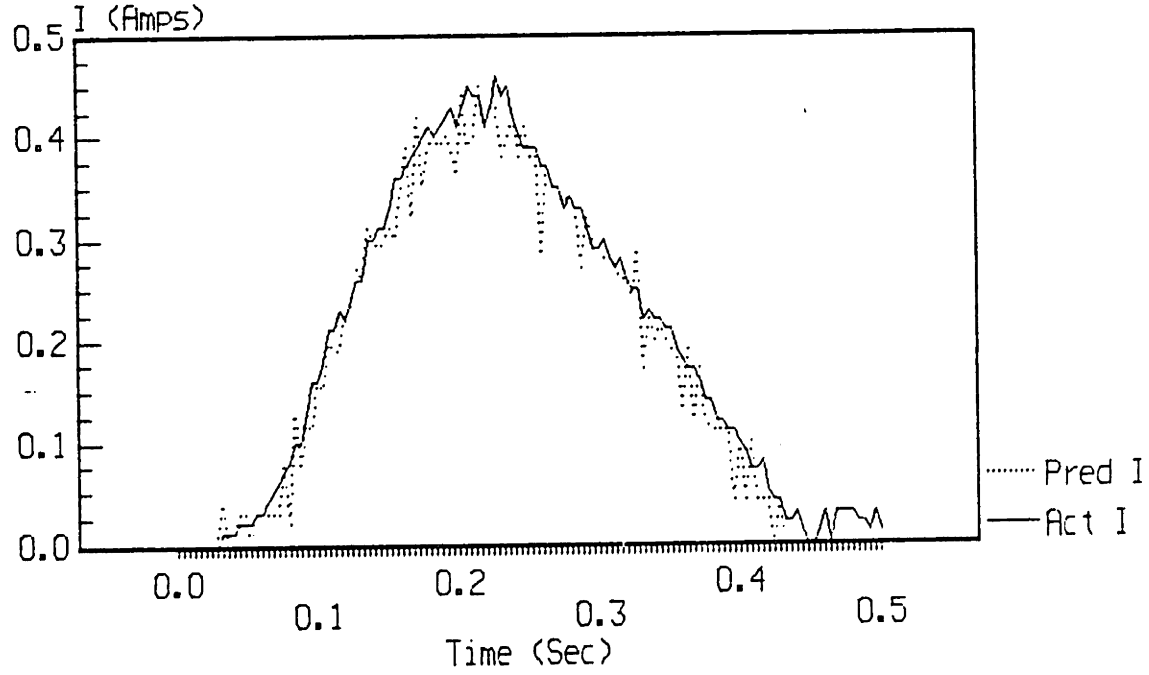

Figure 5-6C
IMPEDANCE REGULATOR UNCONTROLLABILITY
Capacitor Voltage Vs. Time

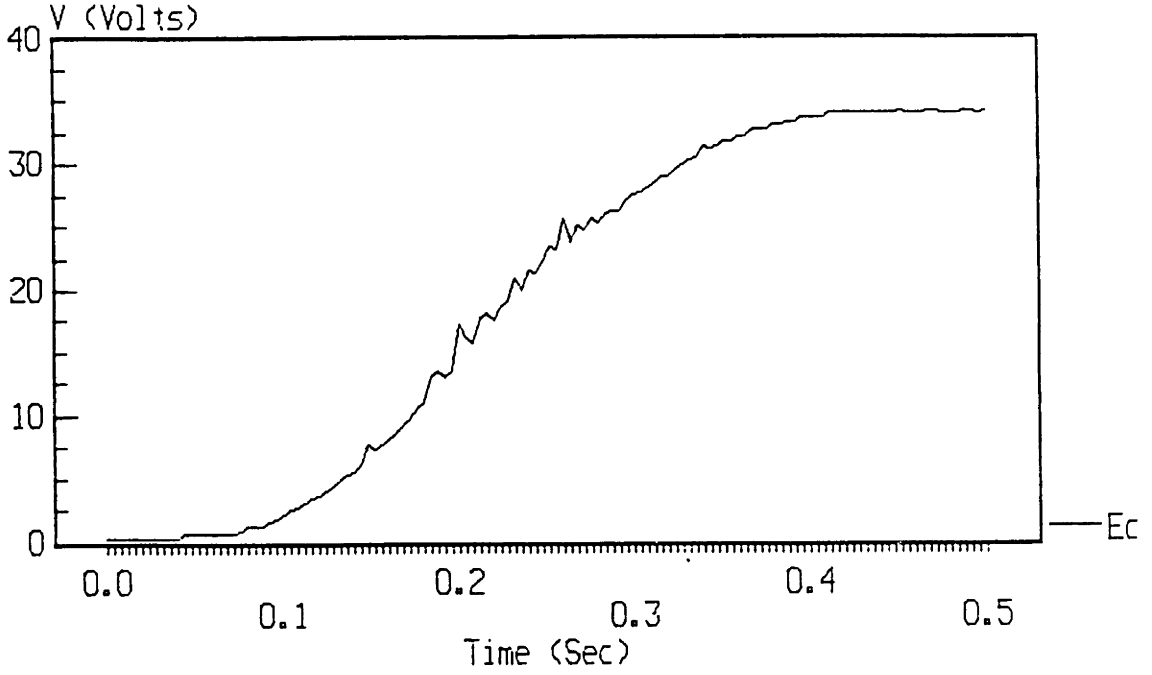

Figure 5-6D
IMPEDANCE REGULATOR UNCONTROLLABILITY
Desired and Actual Knee Impedance
Coefficients

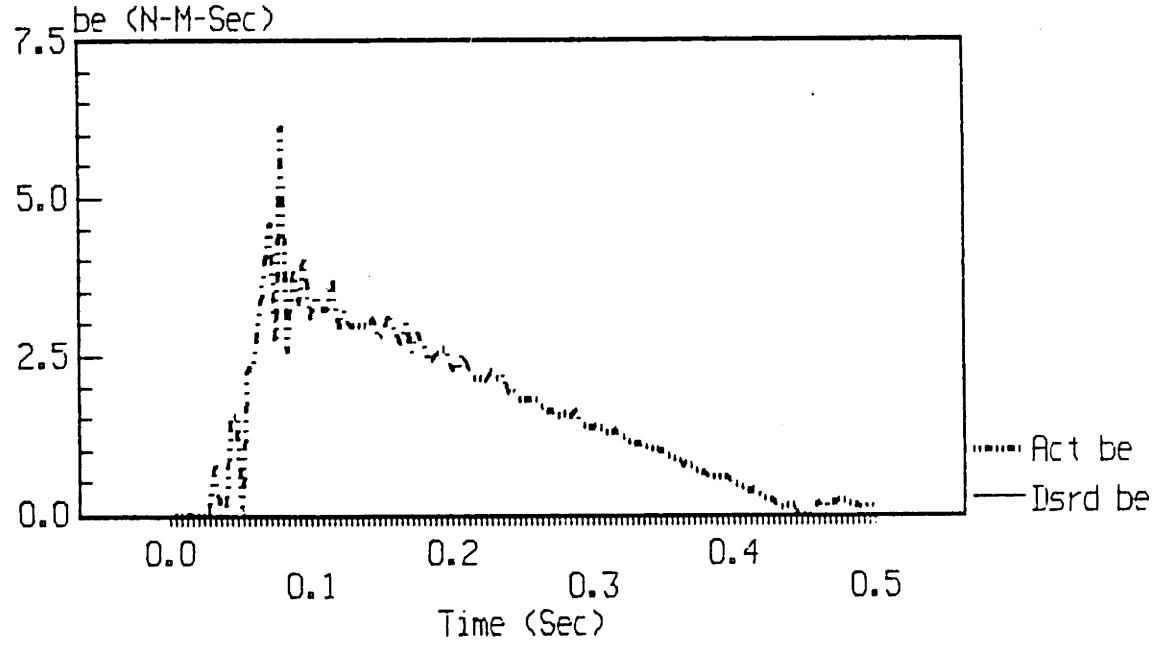

of the entire regenerative knee system. Figure 5-6 illustrates this problem by showing that the controller could not change the amount of motor current when the capacitor voltage was nearly zero. A possible solution to this problem will be presented in the following chapter.

The error due to the nonlinear clipping effect which occurred at high capacitor voltages and low duty cycles will not be presented from experimental data. It was present in the knee system but was not a serious problem. Feedback could be used to eliminate this problem, if desired.

The angular position quantization errors led to quantization errors in the angular velocity. Also random glitches were sometimes present that disturbed the regulator. The quantization noise in angular velocity can make the motor current "noisy" as discussed previously and shown in Figure 5-3. The results of an angular velocity glitch is shown in Figure 5-4. A quadrature-decoding integrated circuit could increase position resolution and nearly eliminate the chances of a glitch--greatly reducing these problems. However, since the mechanical inertia acted like a large low-pass filter, these errors were not very noticeable.

The last of the obvious knee problems started to occur after the data shown in Figure 5-1 to 5-4 was obtained. A large amount of motor current noise was, and still is, present in only one direction of knee rotation and is probably due to bad motor brushes. Large voltages spikes

were very evident when the motor was connected directly to an oscilloscope and then rotated. Bad brushes caused the motor current data to be noisy. The motor current noise was undetectable mechanically because of the comparatively large mechanical inertia. However, if the voltage spikes become too large, the power electronics (the FETs) could be severely damaged.

A measure of regeneration efficiency was obtained by initially placing the leg at a 45 degree angle from vertical and then by letting it rotate freely until it stopped--ending in a vertical position. A SACH foot with shoe was attached to the leg. The impedance regulator was set at various electrical damping coefficients. The starting voltage on the capacitor was set high enough to prevent limiting the efficiency as discussed in chapter 4. The efficiency was then determined by dividing the change of potential energy of the knee system by the amount of energy stored electrically in the energy storage element (the capacitor). The results for the nonoptimal impedance regulator are shown in Figure 5-7. Note that b_m was fixed, so b_n varied with b_e. The predicted efficiency curve shown in Figure 5-7 is the same as the predicted efficiency curve for the nonoptimal regulator shown in Figure 4-2 except plotted against b_e instead of b_n.

The predicted and actual efficiencies differed significantly for two reasons: the knee system contained a large amount (about 1 N-M) of coulombic friction and the

Figure 5-7
ENERGY REGENERATION EFFICIENCIES AS A
FUNCTION OF IMPEDANCE COEFFICIENT
[be(opt) = 1.12 N-M-Sec]

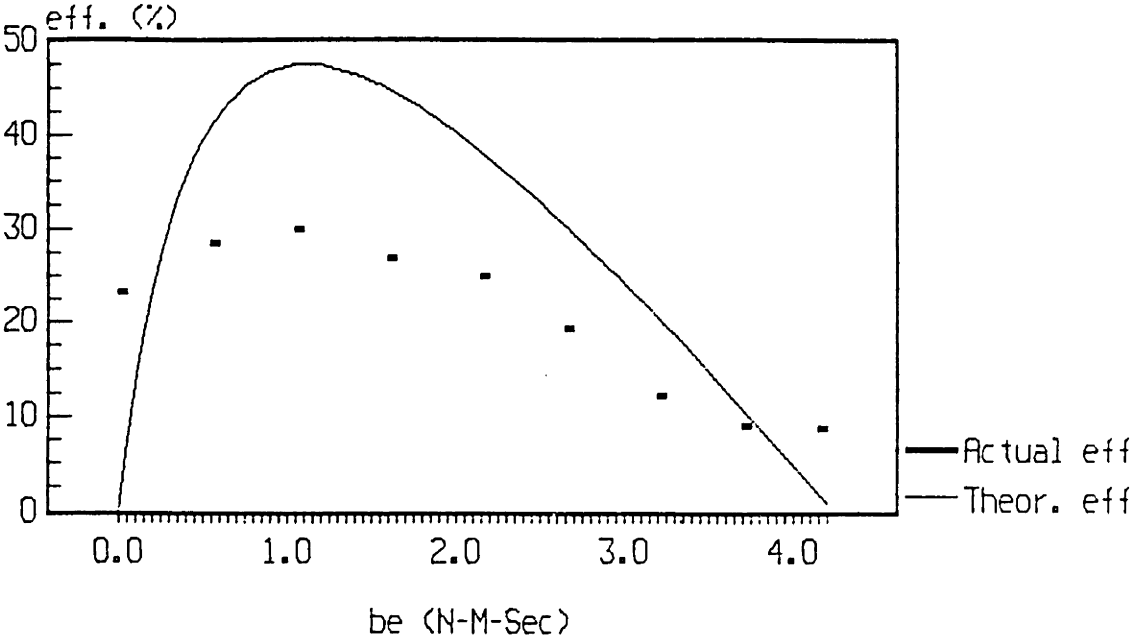

duty cycle was limited to between about 5 and 95% in the real hardware. The coulombic friction reduced the efficiencies for all b_e while the reduced range of duty cycles increased the efficiencies at the extremes. The coulombic friction must be eliminated!

In summary, the nonoptimized impedance regulator functioned very well in some regions of operation from a control standpoint--the electrical impedance coefficient obtained was just what was desired. The actual energy regeneration efficiency was found be much lower than predicted due to coulombic friction. Another serious problem that remained was that the knee was uncontrollable and inefficient at low capacitor voltages.

In the next and final chapter, conclusions will be presented as well as recommendations for further work. A recommended modification to the power electronics will be presented that may fix the uncontrollability and inefficiency problem.

Chapter Six

Conclusions and Recommendations

This final chapter can be divided into three major sections. The first section describes the current state of the regenerative knee--how well the knee functioned as well as its major remaining problems. The second section consists of suggestions for the design of a second generation leg and recommendations for further work. The last section summarizes how a regenerative leg could benefit unilateral above-knee amputees.

In the first chapter, it was stated that the knee should control the swing phase of level walking in an acceptable way as well as simultaneously regenerate as much energy as possible. The nonoptimal impedance regulator did control the knee quite well under many operating conditions. However, when the capacitor was discharged the knee became both uncontrollable and inefficient--the electrical impedance was always maximum, independent of the duty cycle. This was clearly the most significant control problem associated with the knee. (A circuit that may eliminate this problem will be recommended later.)

In terms of energy regeneration, the knee did not function as well as expected. It achieved a maximum efficiency of about 30% instead of the 48% predicted. The difference in efficiencies was probably due to the energy

lost by coulombic friction. The efficiency was also limited when the capacitor voltage was low and the angular velocity was high.

For the regenerative knee to operate more desirably, some very important work must be done. First, the uncontrollability and inefficiency problem of the knee at low capacitor voltages must be eliminated. A circuit that may eliminate this problem will be recommended. Second, the mechanical friction of the knee must be reduced. Then, some suggestions that should follow this work are given.

There appears to be two ways to eliminate the uncontrollability and inefficiency problem of the knee at low capacitor voltages. First of all, the capacitor could always be left charged above about 60V so that this problem is never encountered, but this may not be practical due to the large capacitor required and for safety reasons. Second, a circuit could be designed to add on to or replace the "H" bridge so that the motor current could always be efficiently limited. One such circuit is recommended below.

A circuit that may eliminate the uncontrollability and inefficiency problem at low capacitor voltages is shown in Figure 6-1. A small capacitor is added to the "H" bridge. It quickly charges--creating a voltage which is used to oppose the back-emf of the motor. In this way, the motor current, as well as the electrical impedance coefficient, can be reduced to the desired value. For all practical purposes, the small capacitor charges up instantly. After

FIGURE 6-1: NEW KNEE PROSTHESIS POWER ELECTRONICS

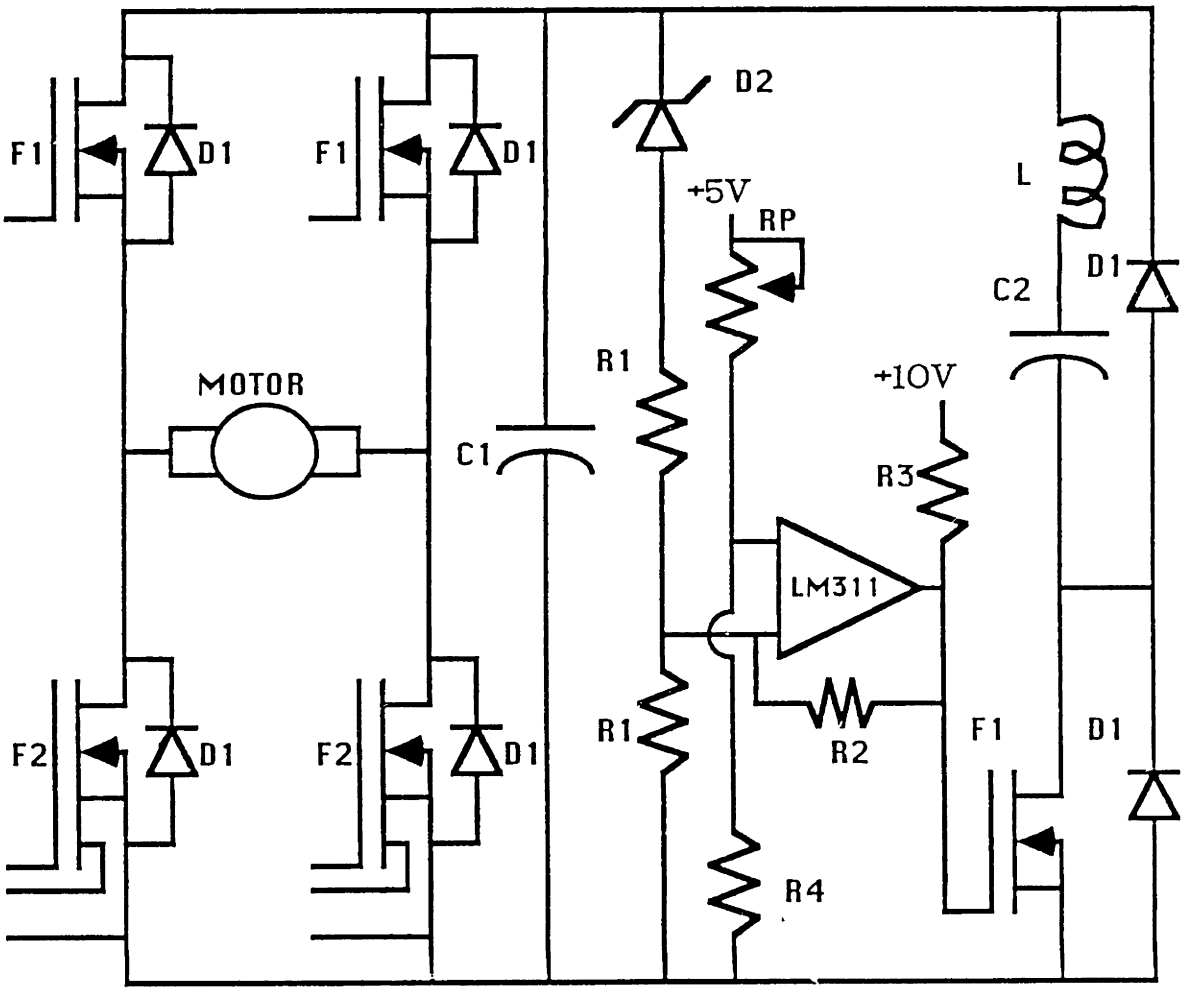

COMPONENT	SPECIFICATIONS	COMPONENT	SPECIFICATIONS
F1	MOSFET	L	1 mH (0.05 Ohm)
F2	SENSEFET (MTP10N10M)	R1	50K
D1	DIODE (IR 50SQ)	R2	225K
D2	ZENER DIODE (60V)	R3	1K
C1	22 MF	R4	2K
C2	2200 MF	RP	10K POT

the small capacitor voltage exceeds about 62V, the comparator turns on the SENSEFET shown in the bottom-right corner of Figure 6-1 and some of the charge on the small capacitor is transferred to the large capacitor (the main storage capacitor). The inductor limits the current between the large and small capacitors. After the small capacitor reaches about 60V, the comparator turns off the SENSEFET and the inductor current flows through the diode shown in the upper-right corner of the figure. In this way, a large voltage is always available to prevent the flow of motor current and the majority of the energy is stored in the large capacitor as before.

If this circuit operates as described, the available electrical impedance coefficients for the impedance regulator can be interpolated from Figure 3-7 or 3-8. The curves for the capacitor voltage in these figures would represent the *small* capacitor voltage, which is always charged to about 60V! Therefore, nearly the entire electrical impedance coefficient range is available immediately--resulting in a knee that is controllable and more efficient! The disadvantages of this circuit include increased complexity, cost, space for the electronics, and possible noise problems. However, when everything is considered, it still should be simple enough to be practical.

A second serious problem with the knee is the large amount of mechanical friction. The linear viscous friction

limits the overall efficiency of the system. However, the coulombic friction not only dissipates energy but it also makes the control problem more difficult. It must be greatly reduced before the knee can approach the efficiencies predicted in chapter 4.

Some research should be conducted to discover the manner in which the magnetic-particle brake should be best used. The particle brake may dissipate more energy than it saves for two reasons. The brake has a significant amount of friction and it is connected to the knee axis by a 36:1 transmission,therefore energy can be dissipated even when the brake is off. Also, electrical energy is used to turn on the brake. It would be best to mechanically disengage the particle brake when not in use. However, it should be noted that even if the brake is not used to optimally regenerate energy, it is desirable for other reasons--to lock the knee in stance, for example.

After the two most serious problems presented above are solved, there is still more work that should be done.

The motor brushes should be replaced since the resulting large voltage spikes could damage the power electronics.

The optimal impedance regulator should be experimentally verified to function as predicted. Also, a controller for the stance phase of level walking should be designed possibly using position feedback. Experimental trials should be conducted with amputees to investigate how

well the knee functions. Different control schemes could be used in swing phase based on the nonoptimal impedance regulator such as position dependent impedance control. It may also prove very interesting to control the knee such that the effective rotational inertia of the leg is the same as a normal while the actual weight is much less (ie. rotational inertia control).

Overall, the regenerative knee could be greatly improved in energy regeneration efficiency and controllability if these suggestions are followed. The back-voltage circuit described in the second section is clearly the most important change necessary to the electrical hardware.

The regenerative knee could possibly benefit unilateral above-knee amputees in several ways. First of all, the new knee may reduce the energy expended by amputees during normal level walking by reducing the vertical movement of their center of gravity--provided that the SACH foot is redesigned. The gait appearance may improve and the stump forces may diminish to a more comfortable level.

In summary, much progress has been made at understanding how the regenerative knee works and what needs to be done to improve it. A regenerative impedance regulator was designed to control the leg acceptably during swing phase while also simultaneously recovering energy. Two major problems remained but possible solutions were proposed for each of them. More work is needed before

experiments with amputees will prove beneficial. The regenerative knee could very well be the leg of the future.

In the end, all of the objectives of this thesis have been obtained but it is clearly evident that there is nothing yet created by man that can even remotely replace the function of the human leg.

REFERENCES

1. Traugh, G.H., et al., "Energy Expenditure of Ambulation in Patients with Above-Knee Amputations," Arch, Phys. Med. Rehab., Vol. 56, Feb. 1975.

2. Bresler, B. and Berry, F.R., "Energy and Power in the Leg During Normal Level Walking," University of California, Berkeley, Series II, Issue 15, Reprint March 1953.

3. Bresler, B., Radcliffe, C.W., and Berry, F.R., "Energy and Power in the Legs of Above-Knee Amputees During Normal Level Walking," Univ. of California, Berkeley, Series II, Issue 31, May 1957.

4. Stein, J.L., "Design Issues in the Stance Phase Control of Above-Knee Prostheses," Ph.D. Thesis, Mechanical Engineering Department, Massachusetts Institute of Technology, pp. 189-190, Jan. 1983.

5. Flowers, W.C., "A Man Interactive Simulator System for Above-Knee Prosthetic Studies," Ph.D. Thesis, Mechanical Engineering Department, Massachusetts Institute of Technology, Aug. 1972.

6. Grimes, D.L., "An Active Multi-Mode Above-Knee Controller," Ph.D. Thesis, Mechanical Engineering Department, Massachusetts Institute of Technology, June 1979.

7. Stein, J.L., "Design Issues in the Stance Phase Control of Above-Knee Prostheses," Ph.D. Thesis, Mechanical Engineering Department, Massachusetts Institute of Technology, Jan. 1983.

8. Grimes, D.L., "An Active Multi-Mode Above-Knee Controller," Ph.D. Thesis, Mechanical Engineering Department, Massachusetts Institute of Technology, p. 23, June 1979.

9. Hunter, B.L., "Design of a Self-Contained, Active, Regenerative Computer Controlled Above-Knee Prosthesis," M.S. Thesis, Mechanical Engineering Department, Massachusetts Institute of Technology, Feb. 1981.

10. Seth, B., "Energy Regeneration and its Application to Active Above-Knee Prostheses," Ph.D. Thesis, Mechanical Engineering Department, Massachusetts Institute of Technology, Feb. 1987.

11. Lampe, D.R., "Design of a Magnetic Particle Brake Above-Knee Prosthesis Simulator System," M.S. and M.E. Thesis, Mechanical Engineering Department, Massachusetts Institute of Technology, pp. 77-80, Feb. 1976.

12. Schechter, S.E., "Passive Self-Contained Microcomputer Controlled Above-Knee Prosthesis," M.S. Thesis, Mechanical Engineering Department, Massachusetts Institute of Technology, May 1986.